

Supporting Information

A symmetry interaction approach to $[M_2L_2]^{4+}$ metallo-cycles and their self-catenation

*Dan Preston,^{*a} Amanda R. Inglis,^a Anna L. Garden,^b and Paul E. Kruger^a*

^a*MacDiarmid Institute for Advanced Materials and Nanotechnology, School of Physical and Chemical Sciences, University of Canterbury, Christchurch 8140, New Zealand*

^b*MacDiarmid Institute for Advanced Materials and Nanotechnology Department of Chemistry, University of Otago, P.O. Box 56, Dunedin*

***daniel.preston@canterbury.ac.nz**

Table of contents

1	Experimental.....	3
1.1	General.....	3
1.2	Precursor synthesis.....	4
1.2.1	Synthesis of 1.....	4
1.3	Ligand synthesis.....	5
1.3.1	Synthesis of L.....	5
1.3.2	Synthesis of L'.....	6
1.4	Complex synthesis.....	7
1.4.1	Synthesis of Pd ₂	8
1.4.2	Synthesis of Pt ₂	11
1.4.3	Synthesis of Pd ₂ '.....	14
1.4.4	Synthesis of Pt ₂ '.....	16
2	Narcissistic self-sorting.....	18
2.1	Palladium(II).....	18
2.2	Platinum(II).....	19
3	Catenation.....	20
3.1	Incomplete conversion to catenane Pd ₂ 'Pd ₂ '.....	20
3.2	Incomplete conversion to catenane Pt ₂ 'Pt ₂ '.....	26
3.3	Mass spectral data.....	31
4	¹ H DOSY NMR data.....	34
4.1	Ligands.....	34
4.2	Palladium(II) complexes.....	35
4.3	Platinum(II) complexes.....	37
5	Computations.....	39
6	References.....	39

1 Experimental

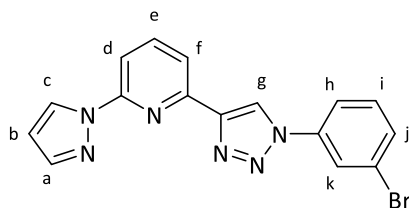
1.1 General

Unless otherwise stated, all reagents were purchased from commercial sources and used without further purification, except for 1-azido-3-bromobenzene,^[1] 2-(1*H*-pyrazol-1-yl)-6-[2-(trimethylsilyl)ethynyl]-pyridine,^[2] 4-(4,4,5,5-tetramethyl-1,3,2-dioxaborolan-2-yl)pyridine,^[3] 3-[4-(4,4,5,5-tetramethyl-1,3,2-dioxaborolan-2-yl)phenyl]pyridine^[4] and [Pt(DMSO)₂Cl₂]^[5] which were synthesised according to literature procedures. Solvents were laboratory reagent grade. Petroleum ether refers to the fraction of petrol boiling in the range 40-60 °C, isopropyl alcohol (IPA), methanol (CH₃OH), dichloromethane (CH₂Cl₂), ethylenediaminetetraacetate (EDTA), ethynyltrimethylsilane (TMS-acetylene), tetrahydrofuran (THF), dimethyl sulfoxide (DMSO), dimethylformamide (DMF). ¹H and ¹³C NMR spectra were recorded on either a 400 MHz Varian 400-MR or Varian 500 MHz AR spectrometer. Chemical shifts are reported in parts per million and referenced to residual solvent peaks (CDCl₃: ¹H δ 7.26 ppm, ¹³C δ 77.16 ppm; *d*₆-DMSO: ¹H δ 2.50 ppm; ¹³C δ 39.52 ppm). Coupling constants (*J*) are reported in Hertz (Hz). Standard abbreviations indicating multiplicity were used as follows: m = multiplet, q = quartet, quin = quintet, t = triplet, dt = double triplet, d = doublet, dd = double doublet, s = singlet, br = broad. Electrospray mass spectra (ESMS) were collected on a Bruker micrOTOF-Q spectrometer.

CAUTION: Azides are explosive and care should be taken when handling them. Reactions were carried out on small scale. No problems were encountered during the course of this work.

1.2 Precursor synthesis

1.2.1 Synthesis of 1



To a mixture of 2-(1H-pyrazol-1-yl)-6-[2-(trimethylsilyl)ethynyl]-pyridine^[2] (454 mg, 1.88 mmol), Na₂CO₃ (797 mg, 7.52 mmol), CuSO₄·5H₂O (469 mg, 1.88 mmol) and ascorbic acid (662 mg, 3.76 mmol) in 4:1 DMF/water (20 mL) was added 3-azido-bromobenzene (740 mg, 3.7 mmol), made and used without purification as per the literature method.^[1] The reaction was stirred overnight at room temperature. After addition of aqueous 0.1 M EDTA/NH₄OH solution (100 mL) and DCM (50 mL) and stirring vigorously for 1 hour, the organic layer was washed with water (6 x 150 mL) and brine (100 mL) and the solvent removed under vacuum. Purification through chromatography on silica (DCM to 1:10 acetone/DCM) gave the product as a white solid (582 mg, 1.58 mmol, 84%). ¹H NMR (400 MHz, [D₆]DMSO, 298 K) δ : 9.60 (1H, s, H_g), 8.94 (1H, d, *J* = 2.5 Hz, H_c), 8.27 (1H, t, *J* = 1.9 Hz, H_k), 8.12 – 8.06 (2H, m, H_{e,h}), 8.00 (1H, d, *J* = 7.7 Hz, H_f), 7.88 (1H, d, *J* = 8.1 Hz, H_d), 7.85 (1H, br, H_a), 7.74 (1H, d, *J* = 8.1 Hz, H_j), 7.60 (1H, t, *J* = 8.1 Hz, H_i), 6.64 (1H, t, *J* = 1.9 Hz, H_b). ¹³C NMR (100 MHz, [D₆]DMSO, 298 K) δ : 150.6, 147.9, 147.7, 142.5, 140.8, 137.6, 131.9, 131.7, 127.5, 122.6, 122.5, 122.4, 119.2, 117.1, 110.9, 108.2. HR ESI-MS (CDCl₃/MeOH) *m/z* = 367.0303 [MH]⁺ (calc. for C₁₆H₁₂BrN₆, 367.0301). IR ν (cm⁻¹) 3137 3096 1572 1485 1460 1435 1030 804 778.

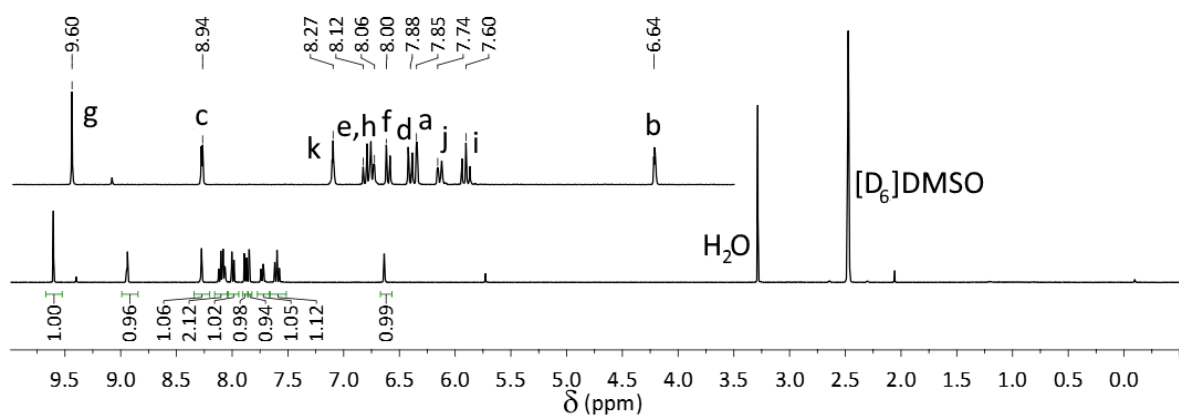


Figure 1.1 ¹H NMR spectrum (400 MHz, [D₆]DMSO, 298 K) of 1.

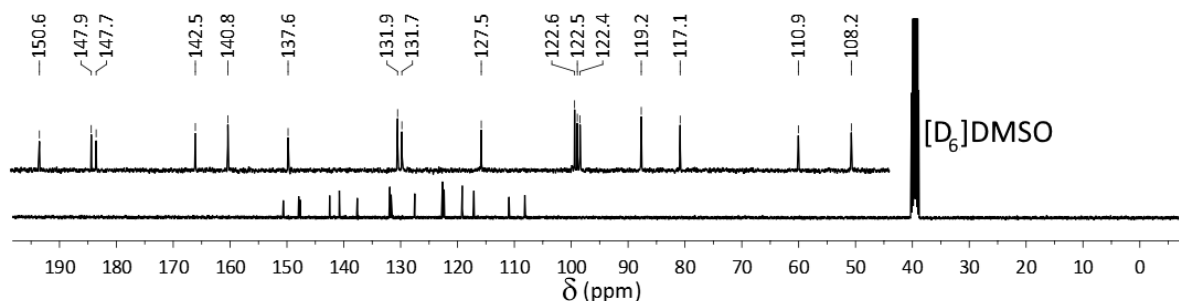
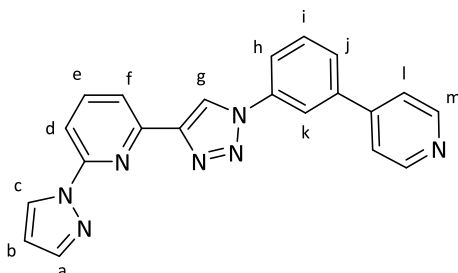


Figure 1.2 ¹³C NMR spectrum (100 MHz, [D₆]DMSO, 298 K) of 1.

1.3 Ligand synthesis

1.3.1 Synthesis of L



A 2:1 DMF/water solution (12 mL) was degassed with nitrogen for 2 hours. Against a positive nitrogen flow, **1** (350 mg, 0.95 mmol), 4-(4,4,5,5-tetramethyl-1,3,2-dioxaborolan-2-yl)pyridine (250 mg, 1.22 mmol),^[3] Na₂CO₃ (777 mg, 7.33 mmol) and [Pd(PPh₃)₄] (54 mg, 4.7 μmol) were added, and the system purged with nitrogen for an additional hour. The reaction was stirred under a nitrogen atmosphere at 140 °C overnight. After addition of DCM (50 mL) and water (100 mL), the organic layer was washed with water (5 x 100 mL) and brine (100 mL). After removal of the solvent under vacuum, the residue was purified through column chromatography on silica (DCM to 1:4 acetone/DCM) to give a white powder. The powder was washed with diethyl ether, then dried under vacuum to give the product as a white solid (225 mg, 0.613 mmol, 65%). ¹H NMR (400 MHz, [D₆]DMSO, 298 K) δ: 9.65 (1H, s, H_g), 8.93 (1H, d, *J* = 2.5 Hz, H_c), 8.71 (2H, d, *J* = 6.0 Hz, H_m), 8.40 (1H, s, H_k), 8.15 – 8.09 (2H, m, H_{e,h}), 8.02 (1H, d, *J* = 7.2 Hz, H_d), 7.96 (1H, d, *J* = 7.9 Hz, H_j), 7.90 – 7.85 (4H, m, H_{a,f,i}), 7.78 (1H, t, *J* = 8.0 Hz, H_l), 6.64 (1H, t, *J* = 2.4 Hz, H_b). ¹³C NMR (100 MHz, [D₆]DMSO, 298 K) δ: 150.7, 150.4, 148.1, 147.6, 145.7, 142.5, 140.7, 139.0, 137.3, 130.9, 127.5, 127.3, 122.4, 121.5, 120.9, 118.5, 117.2, 110.9, 108.2. HR ESI-MS ([D₆]DMSO/DCM/MeOH) *m/z* = 366.1472 [MH]⁺ (calc. for C₂₁H₁₆N₇, 366.1462). IR ν (cm⁻¹) 3128 3086 1591 1390 790 752.

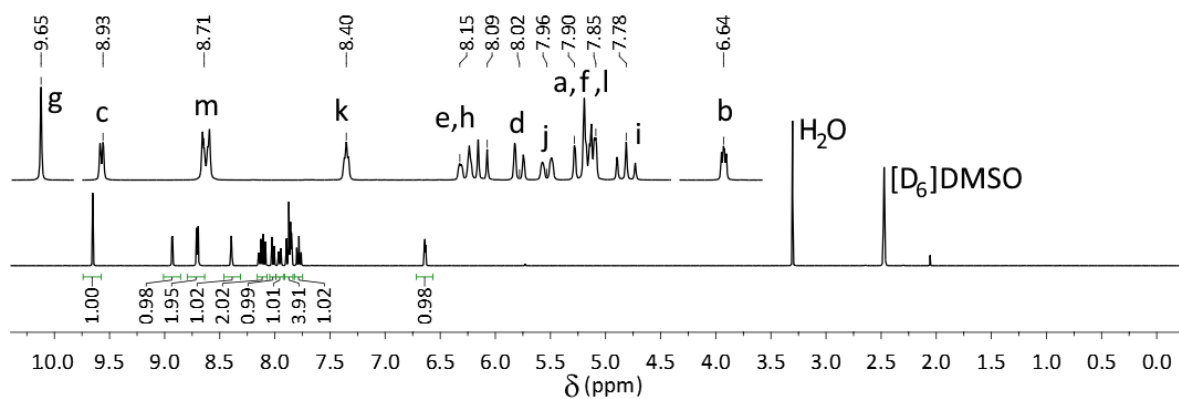


Figure 1.3 ¹H NMR spectrum (400 MHz, [D₆]DMSO, 298 K) of L.

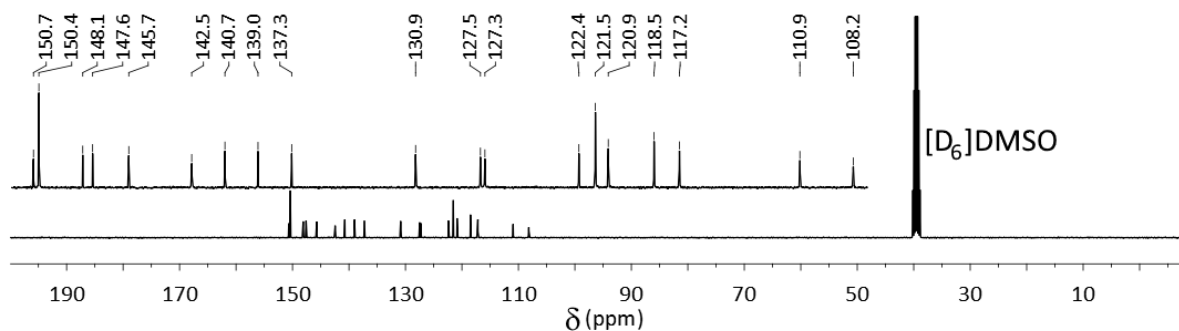
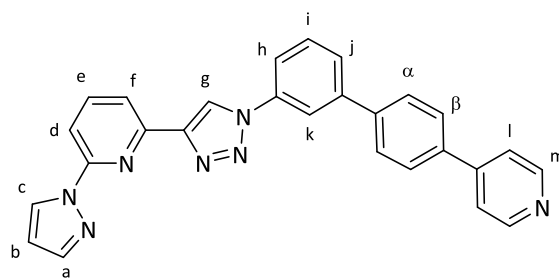


Figure 1.4 ¹³C NMR spectrum (100 MHz, [D₆]DMSO, 298 K) of L.

1.3.2 Synthesis of L'



A 2:1 DMF/water solution (12 mL) was degassed with nitrogen for 2 hours. Against a positive nitrogen flow, **1** (120 mg, 0.33 mmol), 3-[4-(4,4,5,5-tetramethyl-1,3,2-dioxaborolan-2-yl)phenyl]pyridine (280 mg, 0.66 mmol),^[4] Na₂CO₃ (279 mg, 2.63 mmol) and [Pd(PPh₃)₄] (19 mg, 1.6 μmol) were added, and the system purged with nitrogen for an additional hour. The reaction was stirred under a nitrogen atmosphere at 140 °C overnight. After addition of DCM (50 mL) and water (100 mL), the organic layer was washed with water (5 x 100 mL) and brine (100 mL). After removal of the solvent under vacuum, the residue was purified through column chromatography on silica (DCM to 1:4 acetone/DCM) to give a white powder. The powder was washed with diethyl ether, then dried under vacuum to give the product as a white solid (97 mg, 0.22 mmol, 67%). ¹H NMR (400 MHz, [D₆]DMSO, 298 K) δ: 9.66 (1H, s, H_g), 8.94 (1H, d, *J* = 2.1 Hz, H_c), 8.64 (2H, d, *J* = 5.8 Hz, H_m), 8.34 (1H, s, H_k), 8.10 (1H, t, *J* = 7.8 Hz, H_e), 8.05 (1H, d, *J* = 8.8 Hz, H_h), 8.02 (1H, d, *J* = 7.2 Hz, H_d), 7.98 – 7.95 (4H, m, H_{α,β}), 7.87 – 7.82 (2H, m, H_{f,j}), 7.84 (1H, d, *J* = 1.5 Hz, H_a), 7.79 (2H, d, *J* = 6.1 Hz, H_i), 7.75 (1H, t, *J* = 7.9 Hz, H_i), 6.63 (1H, t, *J* = 1.7 Hz, H_b). ¹³C NMR (100 MHz, [D₆]DMSO, 298 K) δ: 150.7, 150.4, 148.2, 147.6, 146.3, 142.5, 141.1, 140.8, 139.6, 137.2, 136.9, 130.7, 127.9, 127.6, 127.5, 127.2, 122.4, 121.2, 119.6, 118.4, 117.2, 110.9, 108.2. HR ESI-MS (DMSO/MeOH) *m/z* = 442.1797 [MH]⁺ (calc. for C₂₇H₂₀N₇, 442.1775). IR ν (cm⁻¹) 3071 1591 1392 1026 790.

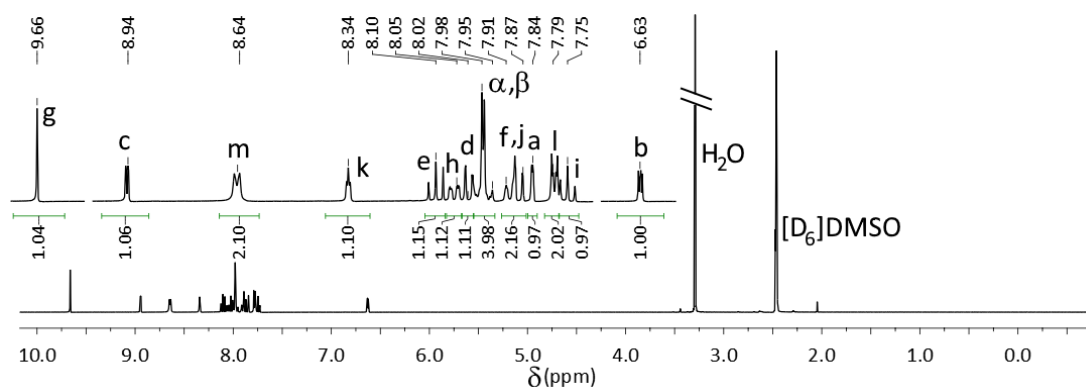


Figure 1.5 ¹H NMR spectrum (400 MHz, [D₆]DMSO, 298 K) of L'.

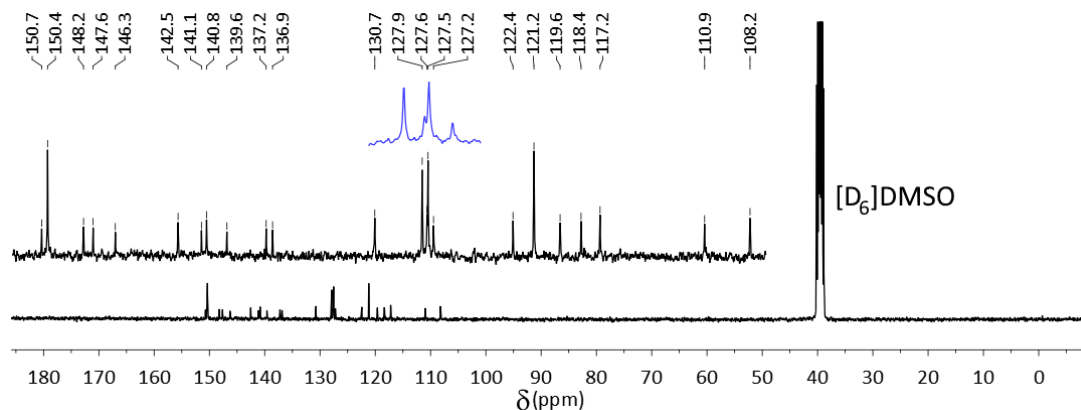


Figure 1.6 ¹³C NMR spectrum (100 MHz, [D₆]DMSO, 298 K) of L'.

1.4 Complex synthesis

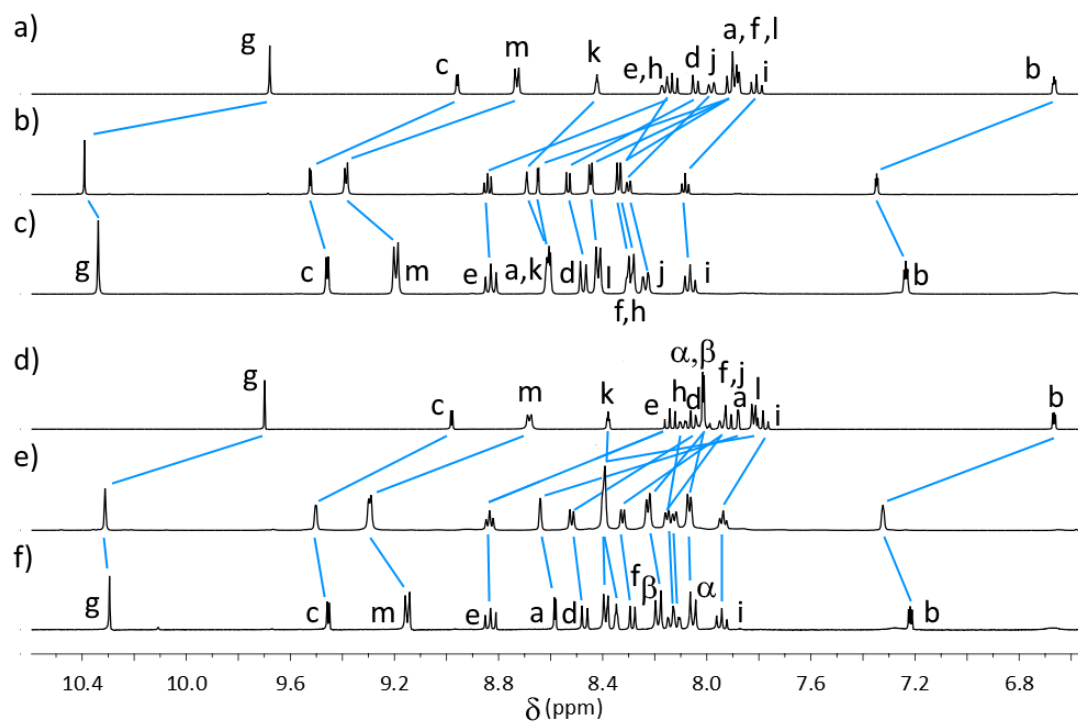
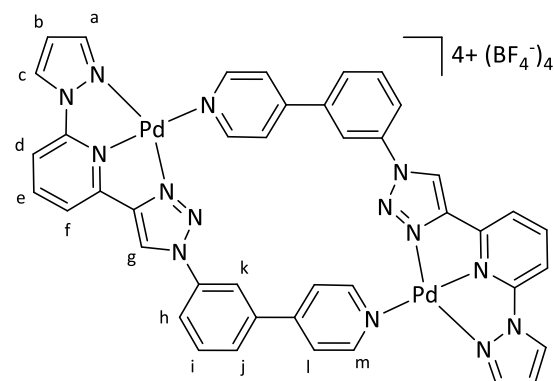


Figure 1.7 Partial stacked ^1H NMR spectra (600 MHz, $[\text{D}_6]$ DMSO, 298 K) at $[\text{ligand}] = 5 \text{ mM}$ for **a) L**, **b) Pt_2** , **c) Pd_2** **d) L'** , **e) Pt_2'** and **f) Pd_2'** .

1.4.1 Synthesis of Pd₂



A solution of $[\text{Pd}(\text{CH}_3\text{CN})_4](\text{BF}_4)_2$ (9.7 mg, 2.2 μmol) in $[\text{D}_6]\text{DMSO}$ (700 μL) was added to **L1** (8.0 mg, 2.2 μmol) and heated gently until a solution was formed. After precipitation with ethyl acetate (5 mL) and centrifugation (4000 RPM, 20 minutes), the pellet was dried under vacuum to give the product as a light yellow solid (12.0 mg, 0.93 mmol, 85%). ^1H NMR (400 MHz, $[\text{D}_6]\text{DMSO}$, 298 K) δ : 10.34 (1H, s, H_g), 9.45 (1H, d, $J = 3.2$ Hz, H_c), 9.19 (2H, d, $J = 6.6$ Hz, H_m), 8.83 (1H, t, $J = 8.2$ Hz, H_e), 8.61 – 8.60 (2H, m, H_{a,k}), 8.46 (1H, d, $J = 5.6$ Hz, H_d), 8.41 (2H, d, $J = 6.7$ Hz, H_i), 8.30 – 2.28 (2H, m, H_{f,h}), 8.25 (1H, d, $J = 8.3$ Hz, H_j), 8.06 (1H, t, $J = 8.0$ Hz, H_i), 7.23 (1H, t, $J = 2.0$ Hz, H_b). ^{13}C NMR (150 MHz, $[\text{D}_6]\text{DMSO}$, 298 K) δ : 153.8, 150.7, 149.8, 148.7, 147.4, 147.2, 145.3, 137.8, 136.8, 135.2, 132.4, 129.9, 125.4, 125.1, 121.5, 120.4, 119.7, 113.2, 111.4. HR ESI-MS (DMF) $m/z = 773.7393$ [$2\text{Pd}_2 + 5\text{BF}_4$] $^{3+}$ (calc. for $\text{C}_{84}\text{H}_{60}\text{B}_3\text{F}_{12}\text{N}_{28}\text{Pd}_4$, 773.7303), 558.5537 [$\text{M} - 2\text{BF}_4$] $^{2+}$ (calc. for $\text{C}_{42}\text{H}_{30}\text{B}_2\text{F}_8\text{N}_{14}\text{Pd}_2$, 558.5468), 236.0218 [$\text{M} - 4\text{BF}_4$] $^{4+}$ (calc. for $\text{C}_{42}\text{H}_{30}\text{N}_{14}\text{Pd}_2$, 236.0212). IR ν (cm^{-1}) 3132 3068 1618 1580 1494 1408 1022 801.

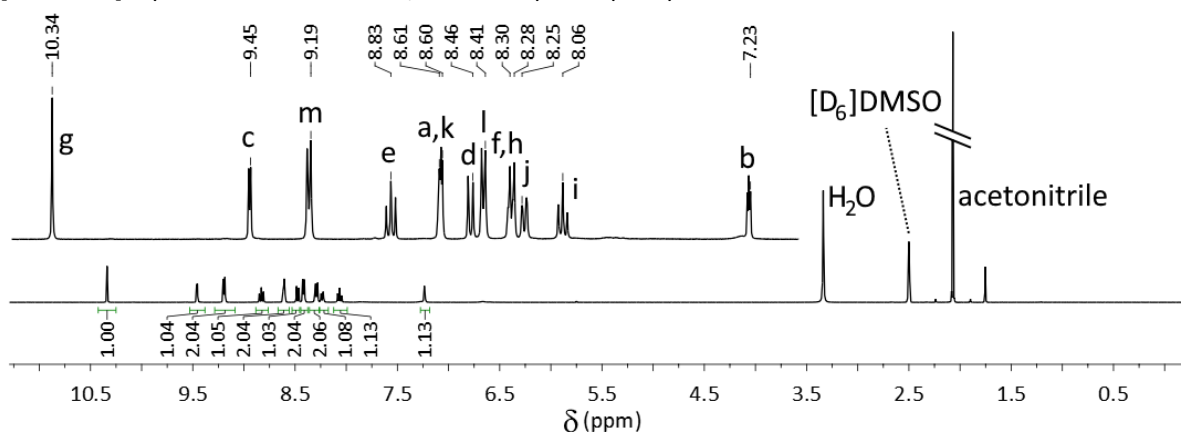


Figure 1.8 ^1H NMR spectrum (400 MHz, $[\text{D}_6]\text{DMSO}$, 298 K) of **Pd₂**.

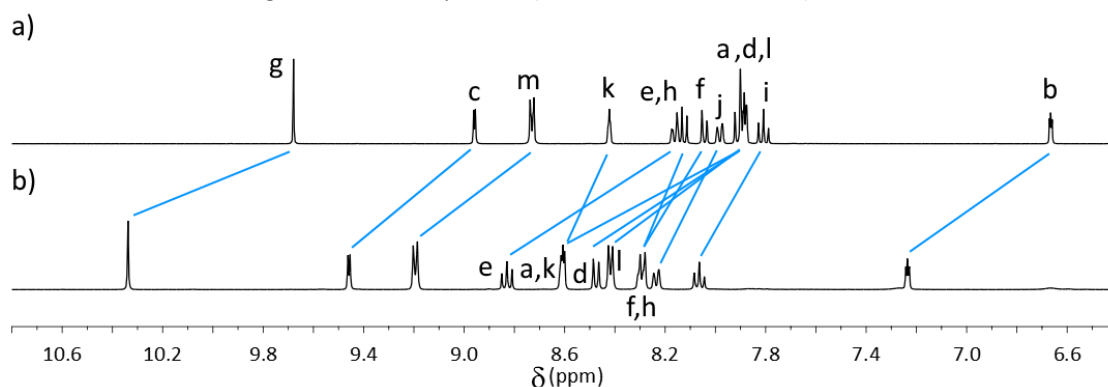


Figure 1.9 Partial stacked ^1H NMR spectra (400 MHz, $[\text{D}_6]\text{DMSO}$, 298 K) of a) **L** and b) **Pd₂**.

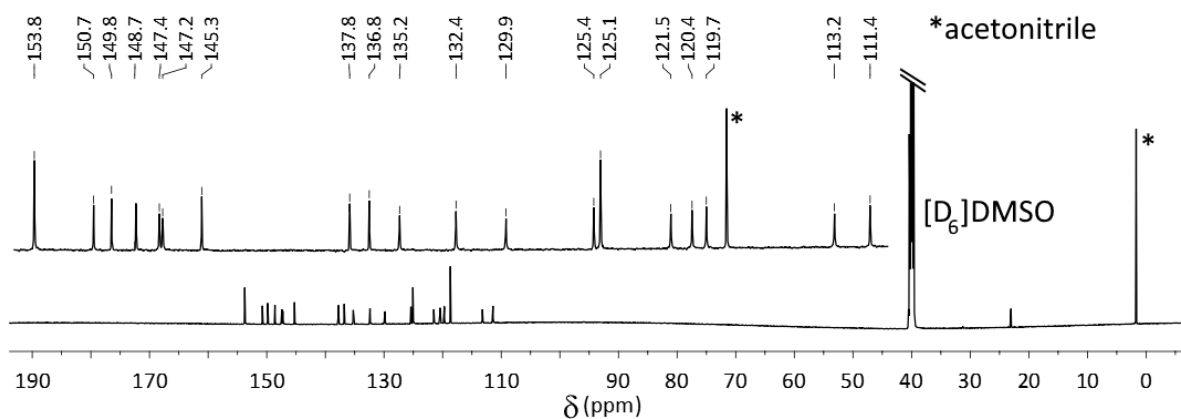


Figure 1.10 ^{13}C NMR spectrum (150 MHz, $[\text{D}_6]\text{DMSO}$, 298 K) of Pd_2 .

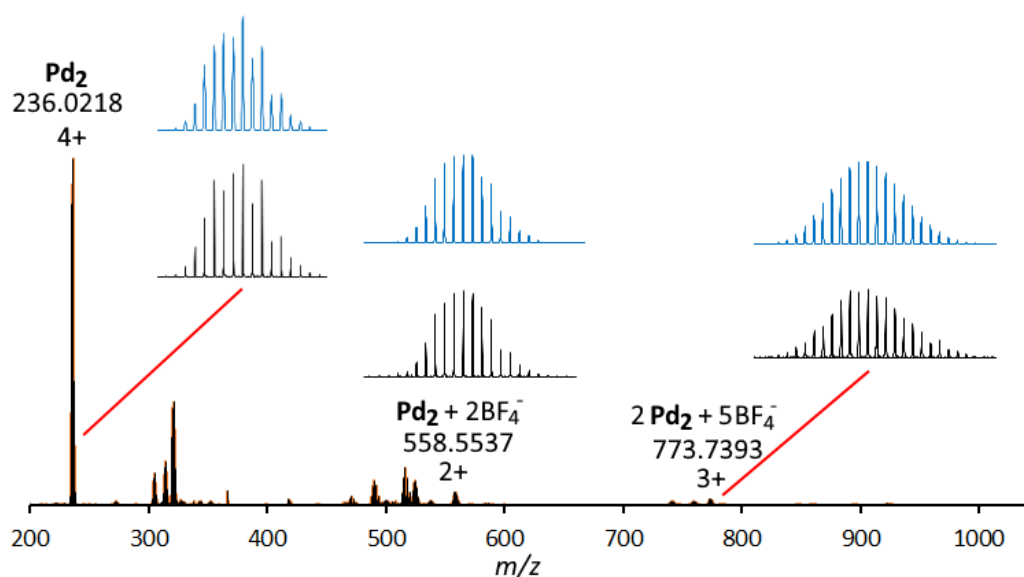


Figure 1.11 Partial mass spectrum (DMSO/DMF) of Pd_2 . Calculated isotopic distributions shown above in blue, observed in black below.

CCDC#: 1951817. Vapour diffusion of diethyl ether into of a DMF solution of Pd_2 gave colourless block crystals of $\text{Pd}_2 \cdot 6\text{DMF}$. X-ray data were collected at 100 K on an Agilent Technologies Supernova system using Cu $\text{K}\alpha$ radiation with exposures over 1.0° , and data were treated using CrysAlisPro^[6] software. The structure was solved using SHELXT within OLEX2 and weighted full-matrix refinement on F^2 was carried out using SHELXL-97^[7] running within the OLEX2^[8] package. All non-hydrogen atoms were refined anisotropically. Hydrogen atoms attached to carbons were placed in calculated positions and refined using a riding model. The structure was solved in the primitive triclinic space group $P\bar{1}$ and refined to an R_1 value of 4.9%.

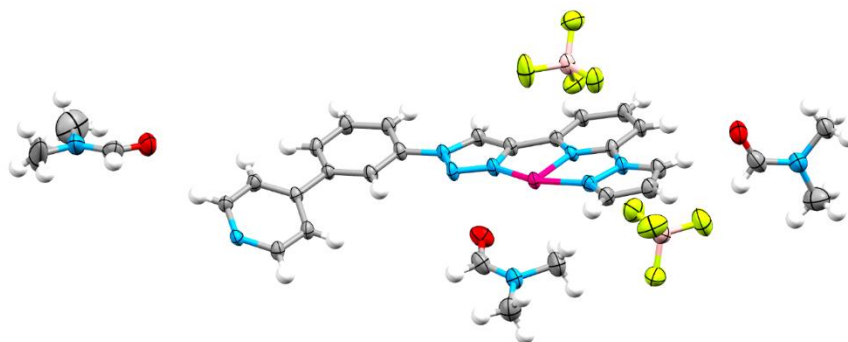
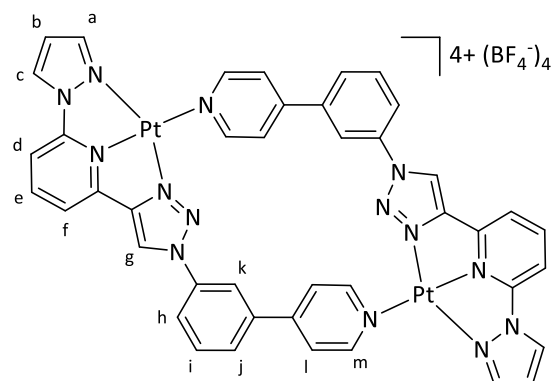


Figure 1.12 Mercury ellipsoid plot of the asymmetric unit of **Pd₂·6DMF**. Ellipsoids shown at 50% probability level. Colour scheme: carbon grey, hydrogen white, boron salmon, fluorine yellow, nitrogen blue, oxygen red, palladium magenta.

Identification code	DP097c	$\rho_{\text{calc}}/\text{cm}^3$	1.607
Empirical formula	$\text{C}_{60}\text{H}_{72}\text{B}_4\text{F}_{16}\text{N}_{20}\text{O}_6\text{Pd}_2$	μ/mm^{-1}	4.996
Formula weight	1729.41	F(000)	876.0
Temperature/K	119.98(11)	Crystal size/ mm^3	$0.295 \times 0.098 \times 0.018$
Crystal system	triclinic	Radiation	$\text{CuK}\alpha$ ($\lambda = 1.54184$)
Space group	P-1	2θ range for data collection/ $^\circ$	8.05 to 145.772
a/ \AA	8.7458(3)	Index ranges	$-10 \leq h \leq 10, -12 \leq k \leq 12, -27 \leq l \leq 27$
b/ \AA	9.9923(3)	Reflections collected	31571
c/ \AA	22.1097(6)	Independent reflections	6981 [$R_{\text{int}} = 0.0997, R_{\text{sigma}} = 0.0625$]
$\alpha/^\circ$	95.966(2)	Data/restraints/parameters	6981/0/493
$\beta/^\circ$	90.358(2)	Goodness-of-fit on F^2	1.032
$\gamma/^\circ$	111.455(3)	Final R indexes [$ I \geq 2\sigma(I)$]	$R_1 = 0.0487, wR_2 = 0.1207$
Volume/ \AA^3	1786.50(10)	Final R indexes [all data]	$R_1 = 0.0610, wR_2 = 0.1310$
Z	1	Largest diff. peak/hole / $e \text{\AA}^{-3}$	1.26/-1.47

1.4.2 Synthesis of Pt₂



A solution of **L** (8.0 mg, 22 μmol) in $[\text{D}_6]\text{DMSO}$ (1 mL) and a solution of $[\text{Pt}(\text{DMSO})_2\text{Cl}_2]^{[5]}$ (9.2 mg, 22 μmol) in $[\text{D}_6]\text{DMSO}$ (1 mL) were added to AgBF_4 (8.5 mg, 44 μmol) and the mixture was heated at 70 $^\circ\text{C}$ in the absence of light for two hours. After centrifugation (4000 RPM, 30 minutes) the filtrate was removed and the pellet discarded. After addition of DMF (2 mL) to the solution, vapour diffusion of diethyl ether into the solution gave the product as a colourless solid (13.1 mg, 8.89 μmol , 82%). ^1H NMR (600 MHz, $[\text{D}_6]\text{DMSO}$, 298 K) δ : 10.39 (1H, s, H_g), 9.53 (1H, d, $J = 2.1$ Hz, H_c), 9.39 (2H, d, $J = 4.3$ Hz, H_m), 8.84 (1H, t, $J = 5.4$ Hz, H_e), 8.69 (1H, s, H_k), 8.65 (1H, d, $J = 1.6$ Hz, H_a), 8.44 (2H, d, $J = 5.6$ Hz, H_l), 8.31 (2H, m, H_{f,h}), 8.08 (1H, t, $J = 5.3$ Hz, H_i), 7.35 (1H, t, $J = 1.6$ Hz, H_b). ^{13}C NMR (150 MHz, $[\text{D}_6]\text{DMSO}$, 298 K) δ : 154.9, 150.9, 150.6, 149.2, 147.8, 147.0, 145.5, 137.5, 136.9, 136.8, 132.5, 129.9, 126.3, 125.4, 121.6, 120.1, 119.8, 112.9, 111.4. HR ESI-MS (DMF) $m/z = 891.8190$ [$2\text{Pt}_2 + 5\text{BF}_4$] $^{3+}$ (calc. for $\text{C}_{84}\text{H}_{60}\text{B}_3\text{F}_{12}\text{N}_{28}\text{Pt}_4$, 891.8092), 647.1109 [$\text{M} - 2\text{BF}_4$] $^{2+}$ (calc. for $\text{C}_{42}\text{H}_{30}\text{B}_2\text{F}_8\text{N}_{14}\text{Pt}_2$, 647.1064), 402.4402 [$\text{M} - 3\text{BF}_4$] $^{3+}$ (calc. for $\text{C}_{42}\text{H}_{30}\text{BF}_4\text{N}_{14}\text{Pt}_2$, 402.4029), 379.7314 [$\text{M} - 4\text{BF}_4 + \text{F}$] $^{3+}$ (calc. for $\text{C}_{42}\text{H}_{30}\text{FN}_{14}\text{Pt}_2$, 379.7347), 280.0453 [$\text{M} - 4\text{BF}_4$] $^{4+}$ (calc. for $\text{C}_{42}\text{H}_{30}\text{N}_{14}\text{Pt}_2$, 280.0510). IR ν (cm^{-1}) 3131 3083 1619 1593 1580 1494 1409 1023 802.

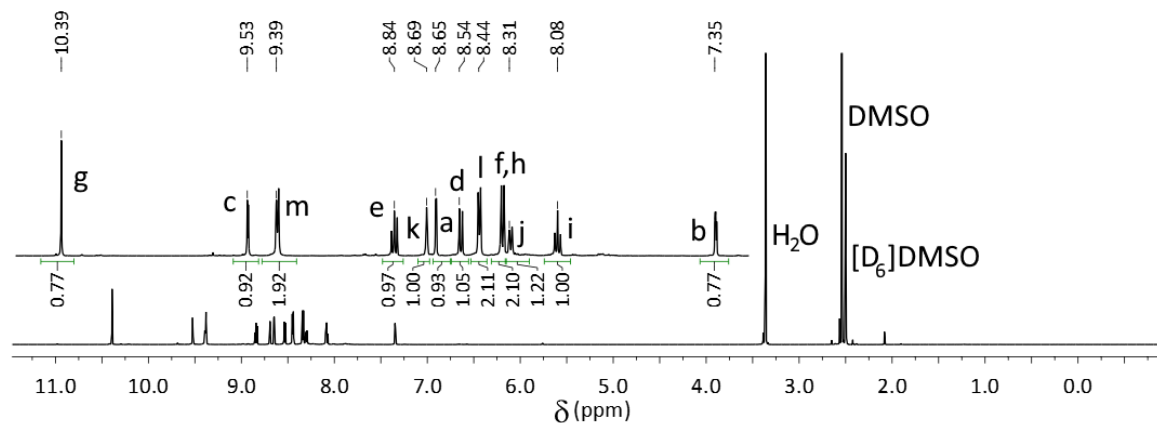


Figure 1.13 ^1H NMR spectrum (600 MHz, $[\text{D}_6]\text{DMSO}$, 298 K) of Pt_2 .

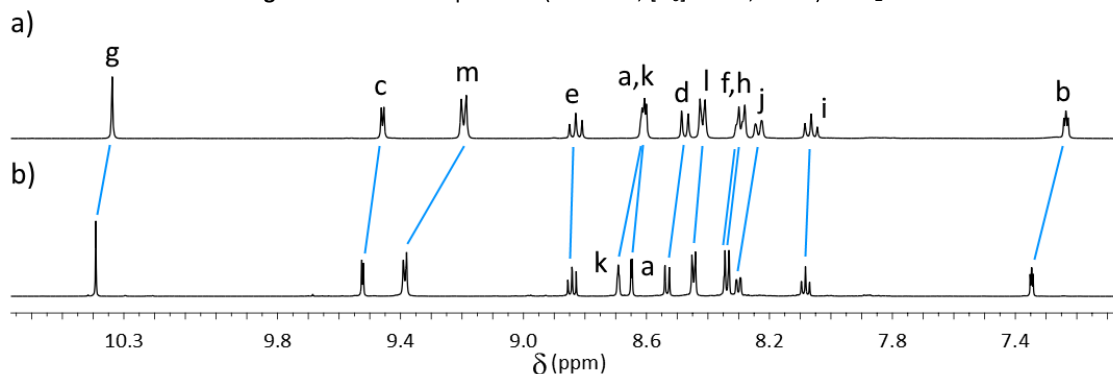


Figure 1.14 Partial stacked ^1H NMR spectra (400 MHz, $[\text{D}_6]\text{DMSO}$, 298 K) of a) Pd_2 and b) Pt_2 .

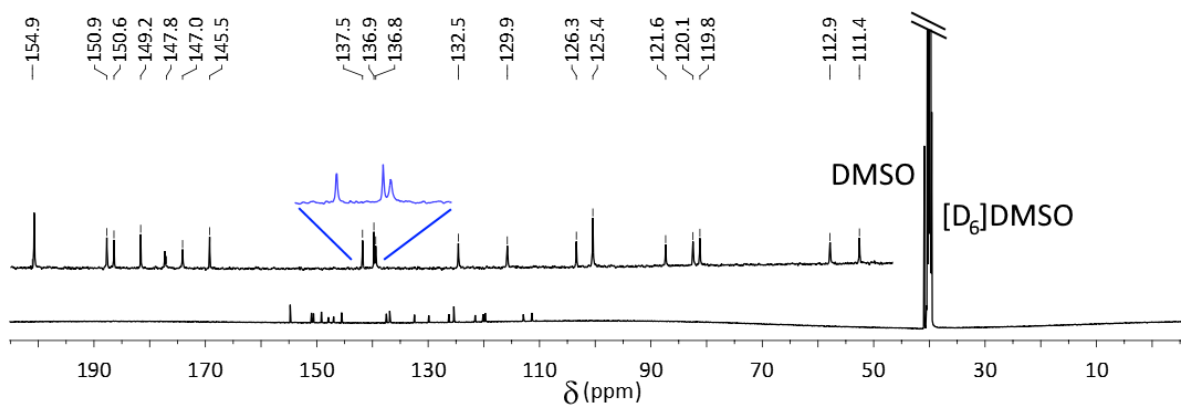


Figure 1.15 ^{13}C NMR spectrum (150 MHz, $[\text{D}_6]\text{DMSO}$, 298 K) of Pt_2 .

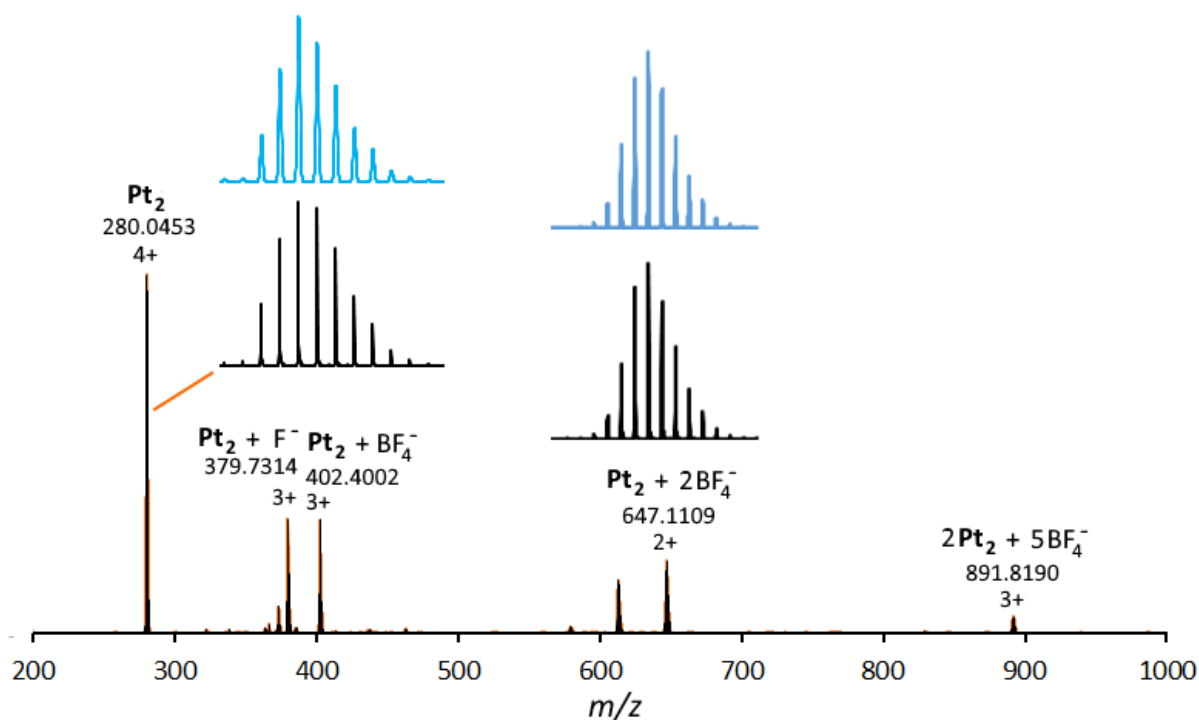


Figure 1.16 Partial mass spectrum (DMSO/DMF) of Pt_2 . Calculated isotopic distributions shown above in blue, observed in black below.

CCDC#: 1951818. Vapour diffusion of diethyl ether into of a DMSO/DMF solution of Pt_2 gave colourless block crystals of $\text{Pt}_2 \cdot 6\text{DMSO}$. X-ray data were collected at 100 K on an Agilent Technologies Supernova system using Cu $\text{K}\alpha$ radiation with exposures over 1.0° , and data were treated using CrysAlisPro^[6] software. The structure was solved using SHELXT within OLEX2 and weighted full-matrix refinement on F^2 was carried out using SHELXL-97^[7] running within the OLEX2^[8] package. All non-hydrogen atoms were refined anisotropically. Hydrogen atoms attached to carbons were placed in calculated positions and refined using a riding model. The structure was solved in the primitive triclinic space group $P-1$ and refined to an R_1 value of 4.5%.

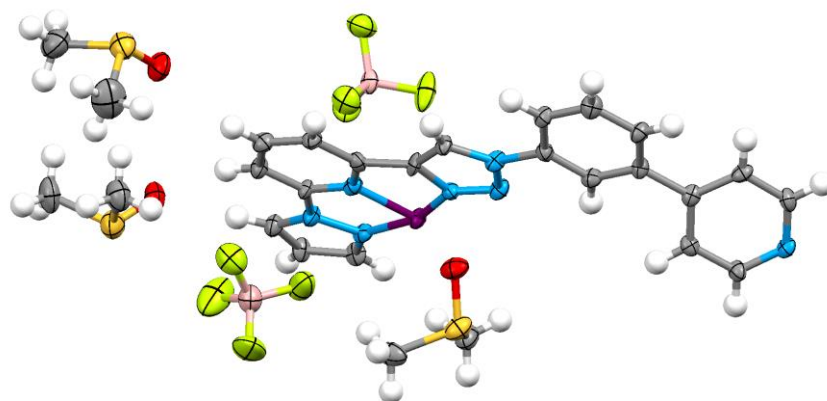
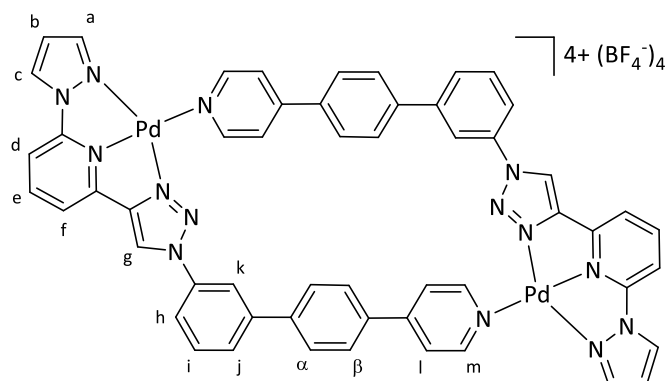


Figure 1.17 Mercury ellipsoid plot of the asymmetric unit of **Pt₂·6DMSO**. Ellipsoids shown at 50% probability level. Colour scheme: carbon grey, hydrogen white, boron salmon, fluorine yellow, nitrogen blue, oxygen red, platinum purple sulphur orange-yellow.

Empirical formula	C ₅₄ H ₆₆ B ₄ F ₁₆ N ₁₄ O ₆ Pt ₂ S ₆	μ/mm^{-1}	9.868
Formula weight	1936.98	F(000)	952.0
Temperature/K	119.99(13)	Crystal size/mm ³	0.102 × 0.079 × 0.017
Crystal system	Triclinic	Radiation	CuK α (λ = 1.54184)
Space group	P-1	2 θ range for data collection/°	8.484 to 122.334
a/Å	8.7843(5)	Index ranges	-9 ≤ h ≤ 9, -11 ≤ k ≤ 9, -23 ≤ l ≤ 23
b/Å	10.4447(6)	Reflections collected	12428
c/Å	21.2945(12)	Independent reflections	5344 [R _{int} = 0.0752, R _{sigma} = 0.0989]
α /°	78.183(5)	Data/restraints/parameters	5344/0/466
β /°	85.140(5)	Goodness-of-fit on F ²	0.989
γ /°	67.156(5)	Final R indexes [I ≥ 2 σ (I)]	R ₁ = 0.0447, wR ₂ = 0.0913
Volume/Å ³	1762.33(19)	Final R indexes [all data]	R ₁ = 0.0643, wR ₂ = 0.1006
Z	1	Largest diff. peak/hole / e Å ⁻³	1.42/-1.43
$\rho_{\text{calc}}/\text{cm}^3$	1.825		

1.4.3 Synthesis of Pd₂'



A solution of $[\text{Pd}(\text{CH}_3\text{CN})_4](\text{BF}_4)_2$ (14 mg, 30 μmol) in DMSO (6 mL) was added to **L'** (14 mg, 30 μmol) and heated gently until a solution was formed. After precipitation with ethyl acetate (20 mL) and centrifugation (4000 RPM, 20 minutes), the pellet was dried under vacuum to give the product as a colourless solid (16 mg, 11 μmol , 73%). Note on the solution phase behaviour on this ligand system: At $[\text{L}'] \leq 5 \text{ mM}$, **Pd₂'** forms. Above this, until the solubility limit of the system ($\sim 100 \text{ mM}$) the catenated form **Pd₂'Pd₂'** is also observed, up until a 4:1 **Pd₂'Pd₂'** / **Pd₂'** ratio. ¹H NMR (400 MHz, [D₆]DMSO, 298 K) δ : 10.29 (1H, s, H_g), 9.45 (1H, d, $J = 3.1 \text{ Hz}$, H_c), 9.16 (2H, d, $J = 6.7 \text{ Hz}$, H_m), 8.83 (1H, t, $J = 8.3 \text{ Hz}$, H_e), 8.58 (1H, d, $J = 2.3 \text{ Hz}$, H_a), 8.47 (1H, d, $J = 8.6 \text{ Hz}$, H_d), 8.40 (2H, d, $J = 6.8 \text{ Hz}$, H_i), 8.35 (1H, s, H_k), 8.28 (1H, d, $J = 7.8 \text{ Hz}$, H_f), 8.20 (2H, d, $J = 8.5 \text{ Hz}$, H_{\beta}), 8.15 – 8.10 (2H, m, H_{h,j}), 8.04 (2H, d, $J = 8.4 \text{ Hz}$, H_{\alpha}), 7.94 (1H, t, $J = 8.0 \text{ Hz}$, H_i), 7.22 (1H, t, $J = 2.8 \text{ Hz}$, H_b). ¹³C NMR (150 MHz, [D₆]DMSO, 298 K) δ : 153.4, 151.3, 149.8, 148.6, 147.5, 145.3, 141.5, 141.2, 136.6, 135.3, 135.2, 131.9, 129.5, 128.9, 128.6, 125.6, 124.4, 120.4, 119.4, 118.8, 113.2, 111.4. HR ESI-MS (DMF) $m/z = 875.4369$ [**2Pd₂'** + 5BF₄]³⁺ (calc. for C₁₀₈H₇₆B₅F₂₀N₅₆Pd₄, 877.1057), 635.0797 [**M** – 2BF₄]²⁺ (calc. for C₅₄H₃₈B₂F₈N₁₄Pd₂, 635.0781), 371.7163 [**M** – 4BF₄ + F]³⁺ (calc. for C₅₄H₃₈FN₁₄Pd₂, 371.7155), 274.0371 [**M** – 4BF₄] (calc. for C₅₄H₃₈N₁₄Pd₂, 274.0369). IR ν (cm⁻¹) 3133 3074 1620 1580 1493 1409 1229 979 802.

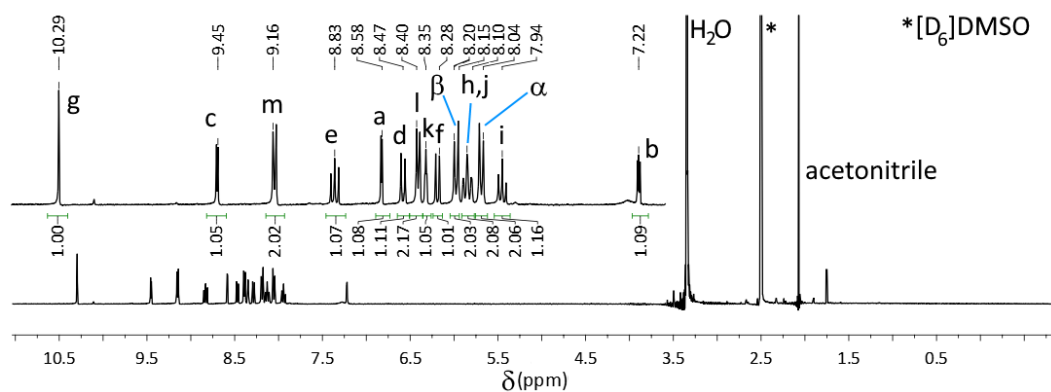


Figure 1.18 ¹H NMR spectrum (400 MHz, [D₆]DMSO, 298 K) of Pd₂'.

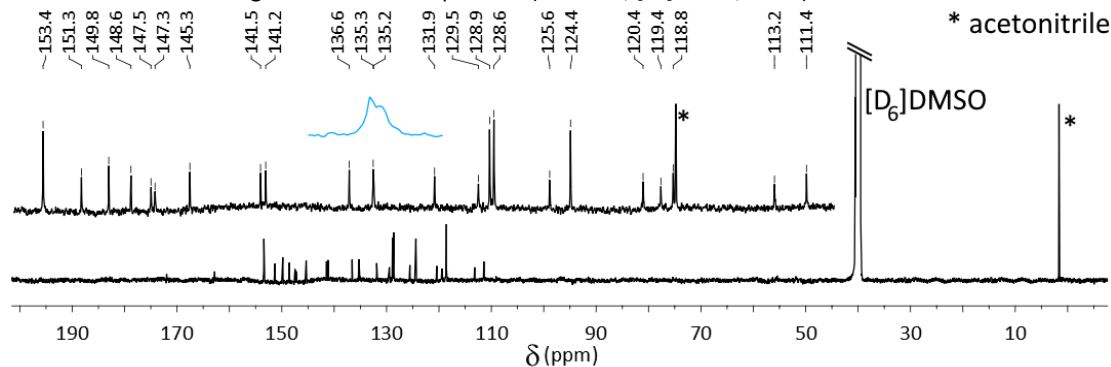


Figure 1.19 ¹³C NMR spectrum (150 MHz, [D₆]DMSO, 298 K) of Pd₂'.

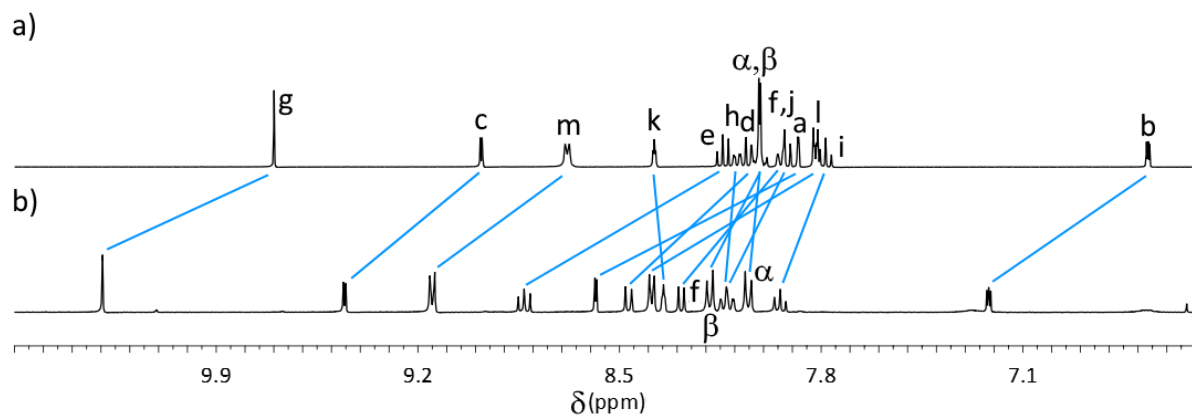


Figure 1.20 Partial stacked ^1H NMR spectra (400 MHz, $[\text{D}_6]\text{DMSO}$, 298 K) of a) **L** and b) **Pd₂'**.

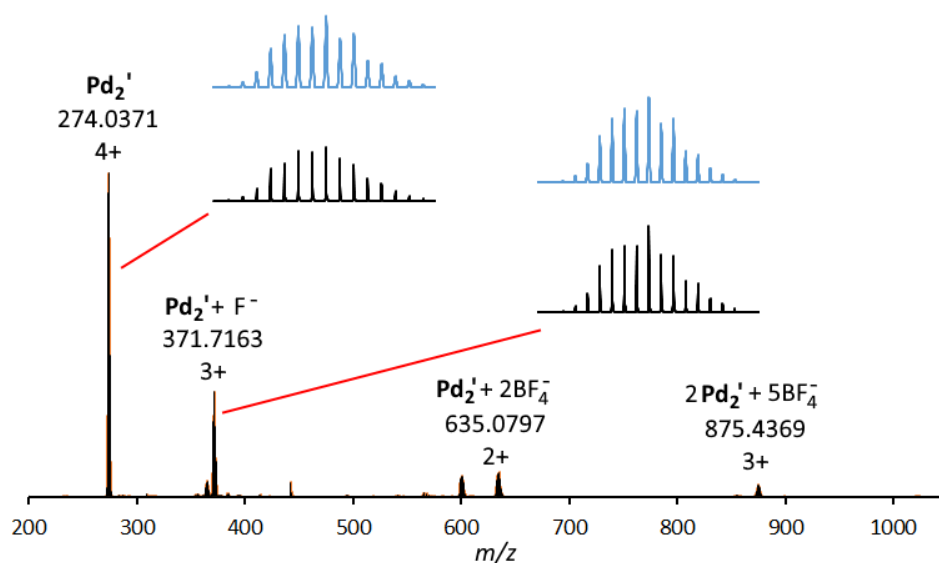


Figure 1.21 Partial mass spectrum (DMSO/DMF) of **Pd₂'**. Calculated isotopic distributions shown above in blue, observed in black below

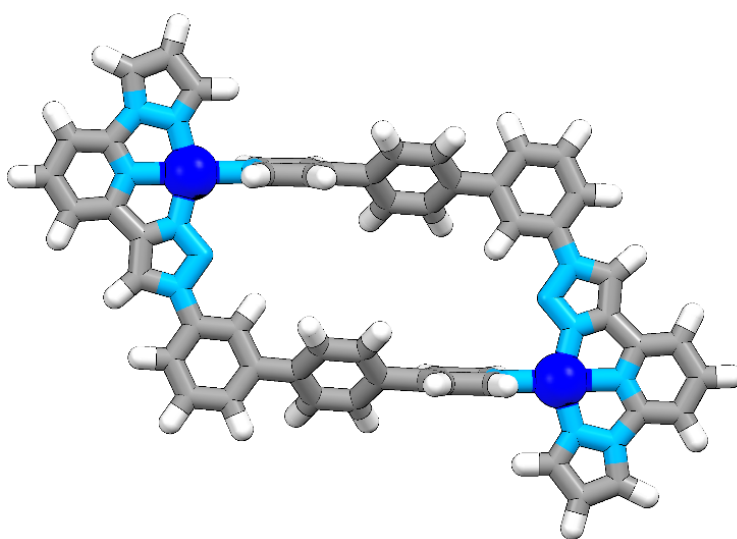
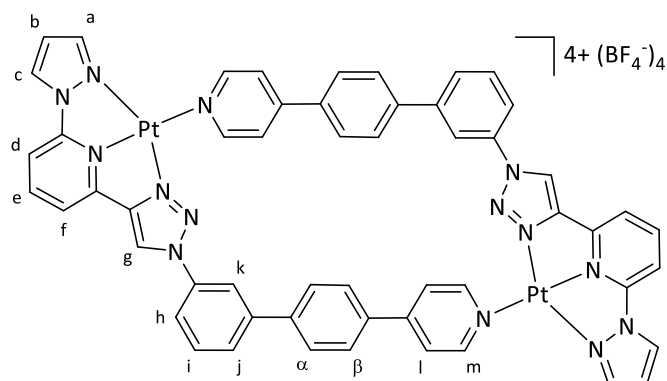


Figure 1.22 Tube depiction of the MMFF^[9] model of **Pd₂'**. Model also available as xyz file.

1.4.4 Synthesis of Pt₂'



A solution of **L'** (14 mg, 32 μmol) in $[\text{D}_6]$ DMSO (500 μL) and a solution of $[\text{Pt}(\text{DMSO})_2\text{Cl}_2]$ (14 mg, 32 μmol) in $[\text{D}_6]$ DMSO (500 μL) were added to AgBF_4 (13 mg, 64 μmol) and the mixture was heated at 70 $^\circ\text{C}$ in the absence of light for two hours. After centrifugation (4000 RPM, 30 minutes) the filtrate was removed and the pellet discarded. After addition of DMF (2 mL) to the solution, vapour diffusion of diethyl ether into the solution gave the product as a colourless solid (15 mg, 10 μmol , 65%). ^1H NMR (600 MHz, $[\text{D}_6]$ DMSO, 298 K) δ : 10.31 (1H, s, H_g), 9.50 (1H, s, H_c), 9.29 (2H, d, $J = 3.6$ Hz, H_m), 8.83 (1H, t, $J = 5.4$ Hz, H_e), 8.64 (1H, s, H_a), 8.51 (1H, d, $J = 5.6$ Hz, H_d), 8.39 (3H, broad, H_{l,k}), 8.32 (1H, d, $J = 5.1$ Hz, H_f), 8.22 (2H, d, $J = 5.2$ Hz, H_{\beta}), 8.16 – 8.12 (2H, m H_{h,j}), 8.06 (2H, d, $J = 5.2$ Hz, H_{\alpha}), 7.94 (1H, t, $J = 5.1$ Hz, H_i), 7.32 (1H, s, H_b). ^{13}C NMR (150 MHz, $[\text{D}_6]$ DMSO, 298 K) δ : 154.0, 150.8, 150.4, 148.7, 147.5, 146.5, 145.2, 140.9, 140.7, 136.3, 136.2, 134.6, 131.5, 129.0, 128.5, 128.1, 125.9, 124.2, 119.6, 118.9, 118.3, 112.4, 110.9. HR ESI-MS (DMSO/DMF) $m/z = 723.1422$ $[\text{M} - 2\text{BF}_4]^{2+}$ (calc. for $\text{C}_{58}\text{H}_{38}\text{B}_2\text{F}_8\text{N}_{14}\text{Pt}_2$, 723.1379), 453.0919 $[\text{M} - 3\text{BF}_4]^{3+}$ (calc. for $\text{C}_{58}\text{H}_{38}\text{BF}_4\text{N}_{14}\text{Pt}_2$, 453.0905), 318.0683 $[\text{M} - 4\text{BF}_4]^{4+}$ (calc. for $\text{C}_{58}\text{H}_{38}\text{N}_{14}\text{Pt}_2$, 318.0667). IR ν (cm^{-1}) 3136 3085 1620 1591 1578 1492 1410 1024 801.

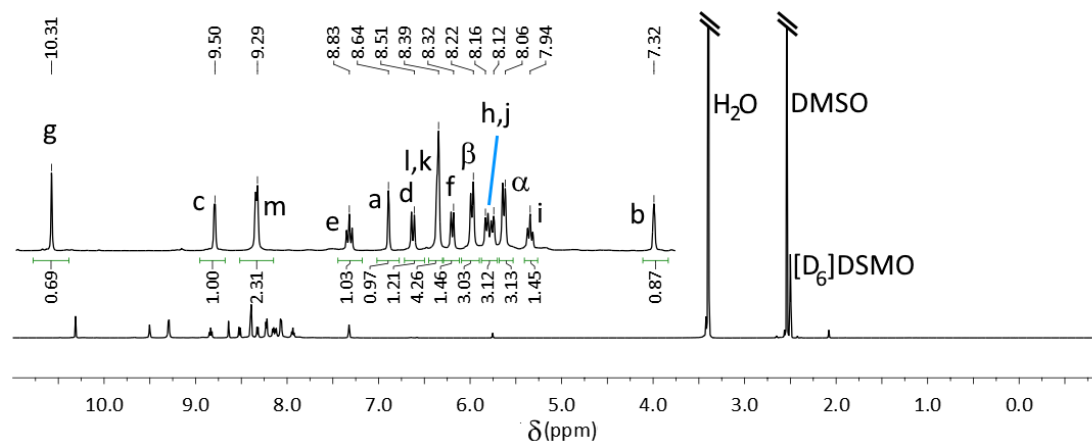


Figure 1.23 ^1H NMR spectrum (600 MHz, $[\text{D}_6]$ DMSO, 298 K) of **Pt₂'**.

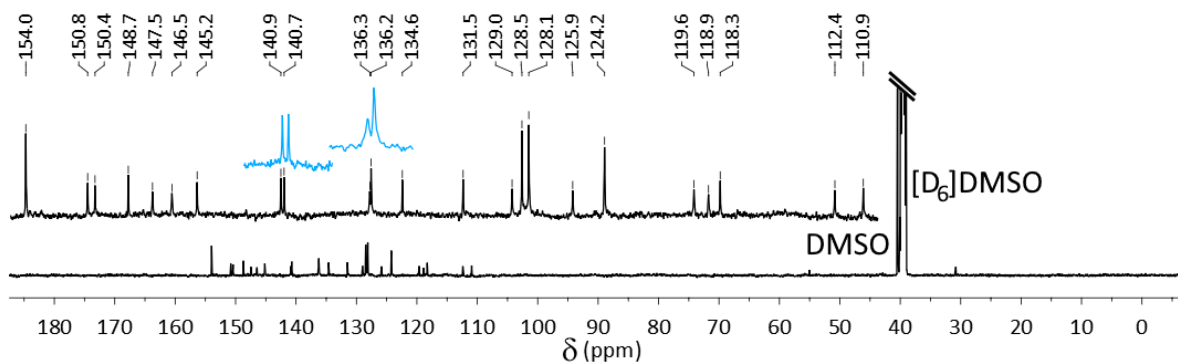


Figure 1.24 ^{13}C NMR spectrum (150 MHz, $[\text{D}_6]$ DMSO, 298 K) of **Pt₂'**.

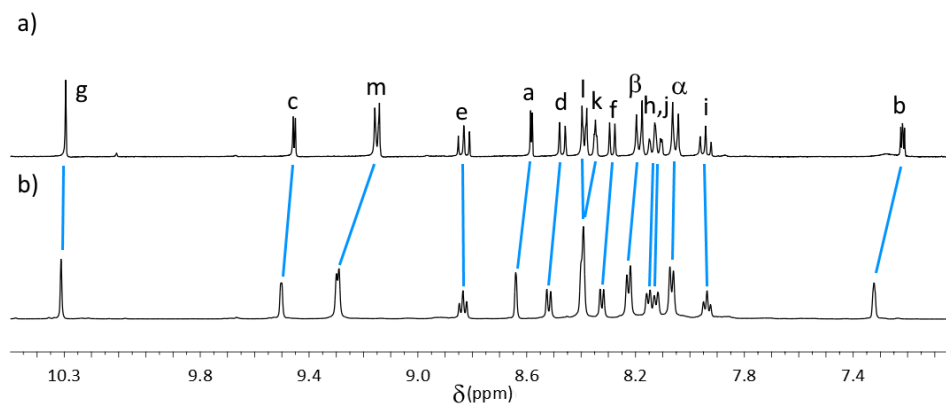


Figure 1.25 Partial stacked ^1H NMR spectra (400 MHz, $[\text{D}_6]\text{DMSO}$, 298 K) of a) Pd_2' and b) Pt_2' .

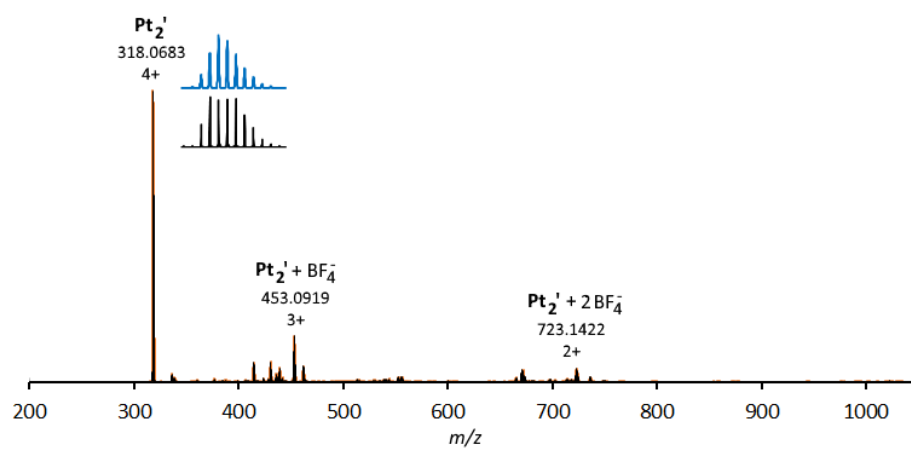


Figure 1.26 Partial mass spectrum (DMSO/DMF) of Pt_2' . Calculated isotopic distributions shown above in blue, observed in black below.

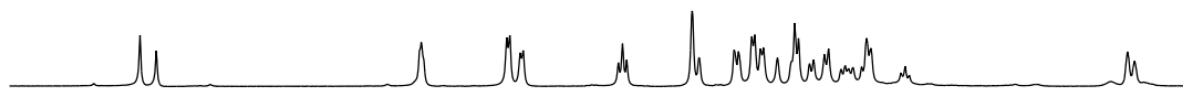
2 Narcissistic self-sorting

2.1 Palladium(II)

a)



b)



c)

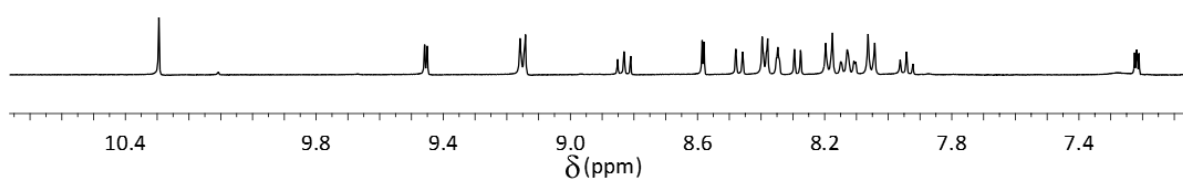


Figure 2.1 Partial stacked ^1H NMR spectra (600 MHz, $[\text{D}_6]\text{DMSO}$, 298 K, in each case, $[\text{ligand}] = 5 \text{ mM}$) of a) Pd_2 , b) Pd_2 and Pd_2' and c) Pd_2' .

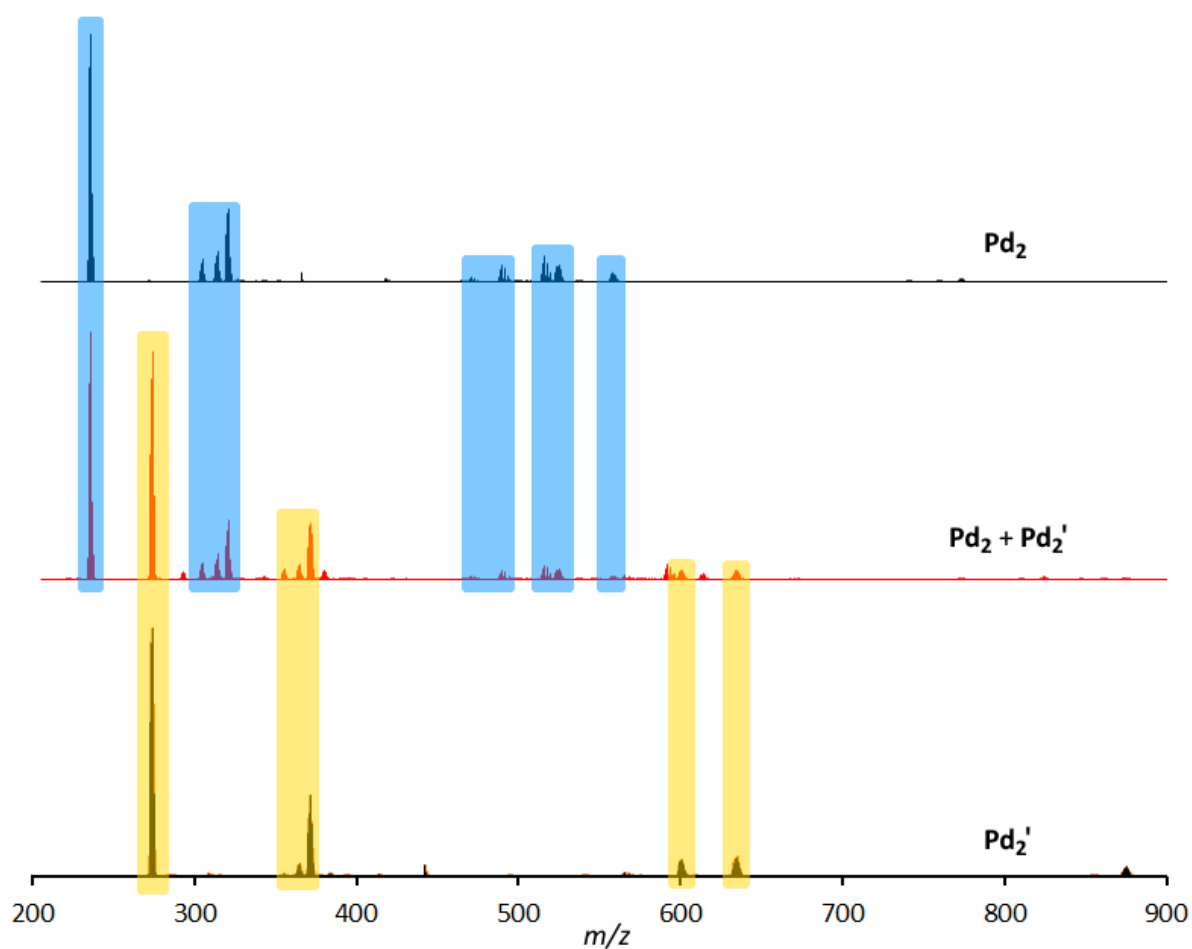


Figure 2.2 Partial mass spectra (DMF) for Pd_2 (above), Pd_2 and Pd_2' (middle) and Pd_2' (below).

2.2 Platinum(II)

a)



b)



c)



10.3 9.9 9.6 9.3 9.0 8.7 8.4 8.1 7.8 7.5
 δ (ppm)

Figure 2.3 Partial stacked ^1H NMR spectra (600 MHz, $[\text{D}_6]$ DMSO, 298 K, in each case, [ligand] = 5 mM) of a) Pt_2 , b) Pt_2 and Pt_2' and c) Pt_2' .

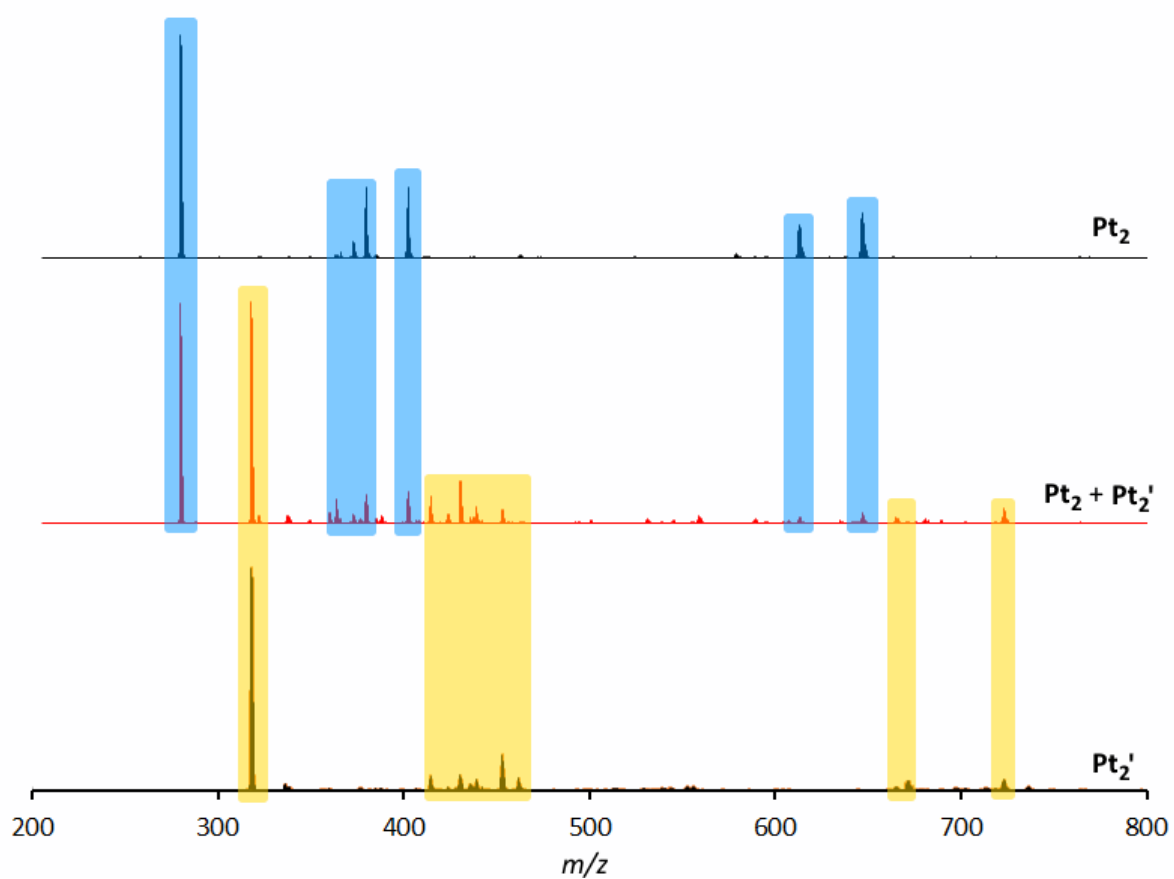


Figure 2.4 Partial mass spectra (DMF) for Pt_2 (above), Pt_2 and Pt_2' (middle) and Pt_2' (below).

3 Catenation

Table 3.1 Maximum observed integrative ratio of catenane to $[M_2L'_2]^{4+}$ via 1H NMR spectroscopy (400 MHz, $[D_6]DMSO$, 298 K).

$[L']$ (mM)	Maximum observed ratio of catenane to $[M_2L'_2]^{4+}$	
	Pd^{II}	Pt^{II}
5	0:1	0:1
30	1:1	1:4
60	2:1	3:7
100	4:1	1:2

3.1 Incomplete conversion to catenane $Pd_2'Pd_2'$

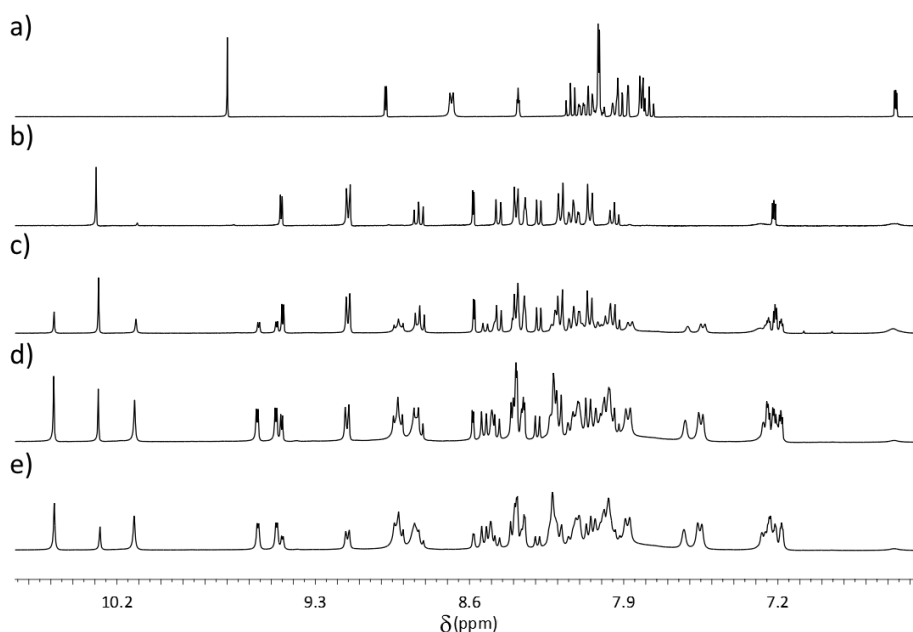


Figure 3.1 Partial stacked 1H NMR spectra (400 MHz, $[D_6]DMSO$, 298 K) of a) L' b) a 2:2 ratio of L'/Pd^{II} at $[L'] = 5$ mM, c) 30 mM, d) 60 mM and e) 100 mM.

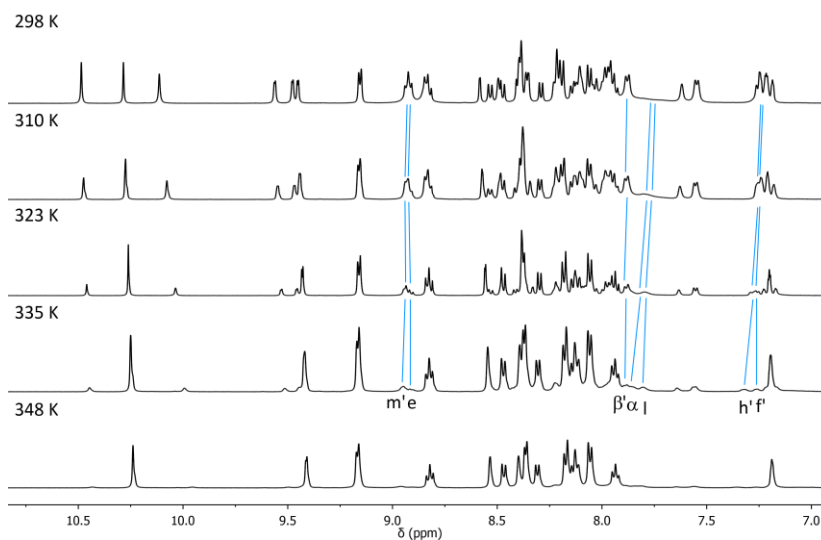


Figure 3.2 Partial stacked 1H NMR spectra (500 MHz, $[D_6]DMSO$) of 2:2 combination of L' and Pd^{II} at $[L'] = 60$ mM at varying temperatures.

Table 3.2 Concentrations of Pd_2' and $\text{Pd}_2'\text{Pd}_2'$ at $[\text{L}'] = 60 \text{ mM}$, as a function of temperature, together with calculated K_{eq} .

Temp (K)	$[\text{Pd}_2']$	$[\text{Pd}_2'\text{Pd}_2']$	K_{eq}
298	9.2	10.4	0.1216
310	13.9	8.0	0.0416
323	19.2	5.4	0.0147
335	24.4	2.8	0.0047
348	27.5	1.2	0.0016

The equilibrium constants above were calculated from:



Note that the value of K_{eq} at 298 K was in agreement from that obtained from averaging K_{eq} at concentrations at which an equilibrium mixture of Pd_2' and $\text{Pd}_2'\text{Pd}_2'$ was observed ($[\text{L}'] = 30, 60$ and 100 mM): 0.123.

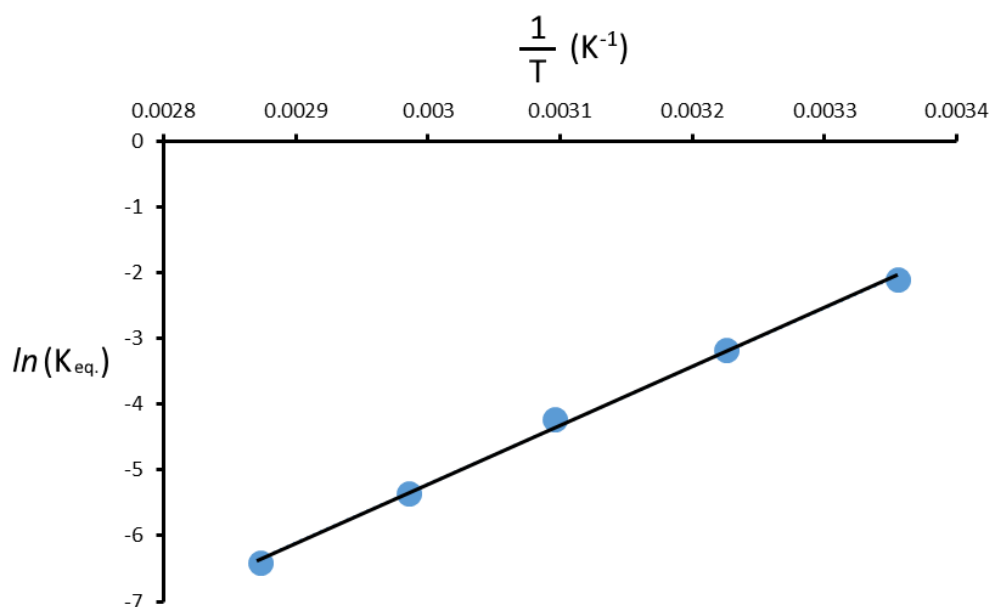


Figure 3.3 van 't Hoff plot for the 2:2 combination of L' and Pd^{II} at $[\text{L}'] = 60 \text{ mM}$. Slope = 8929.9, intercept = -32.022, $R^2 = 0.9976$.

From the plot above:

$$\Delta H = -8.314 \times 8929.9 = 74.2 \text{ kJ mol}^{-1}$$

$$\Delta S = 8.314 \times -32.02 = -266 \text{ J mol}^{-1}$$

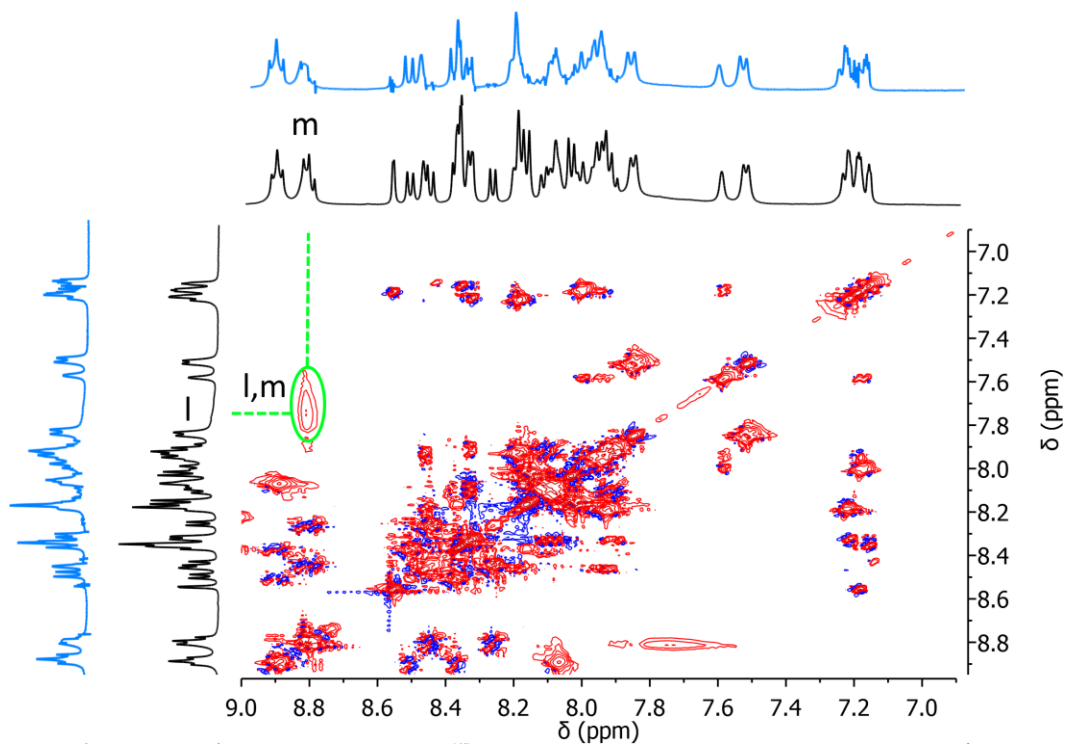


Figure 3.4 Close up ^1H TOCSY spectrum (500 MHz, $[\text{D}_6]$ DMSO, 298 K) from the equilibrium mixture of $\text{Pd}_2'\text{Pd}_2'$ and Pd_2' , confirming through-bond coupling of H_m and H_l . Actual spectrum shown in black, manually subtracted spectrum for $\text{Pd}_2'\text{Pd}_2'$ shown in blue.

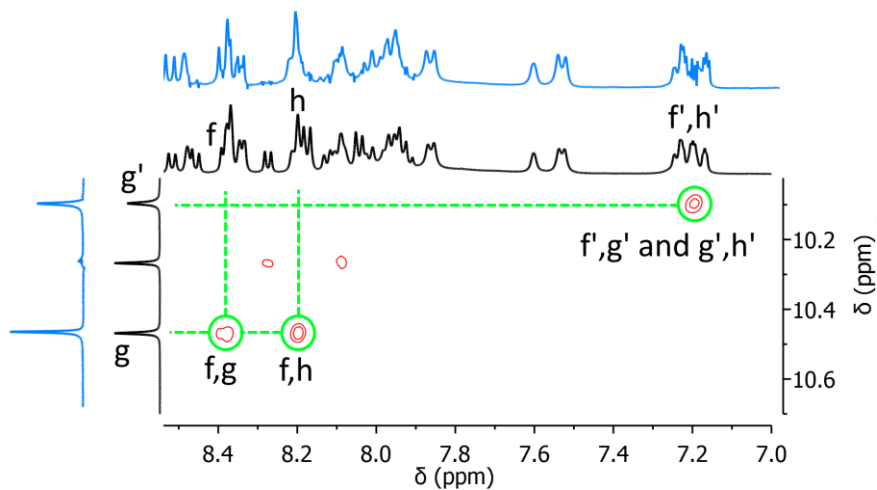


Figure 3.5 Partial ^1H COSY NMR spectrum (500 MHz, $[\text{D}_6]$ DMSO, 298 K) from the equilibrium mixture of $\text{Pd}_2'\text{Pd}_2'$ and Pd_2' , showing COSY couplings between H_g proton environments and H_h and H_h proton environments. Actual spectrum shown in black, manually subtracted spectrum for $\text{Pd}_2'\text{Pd}_2'$ shown in blue.

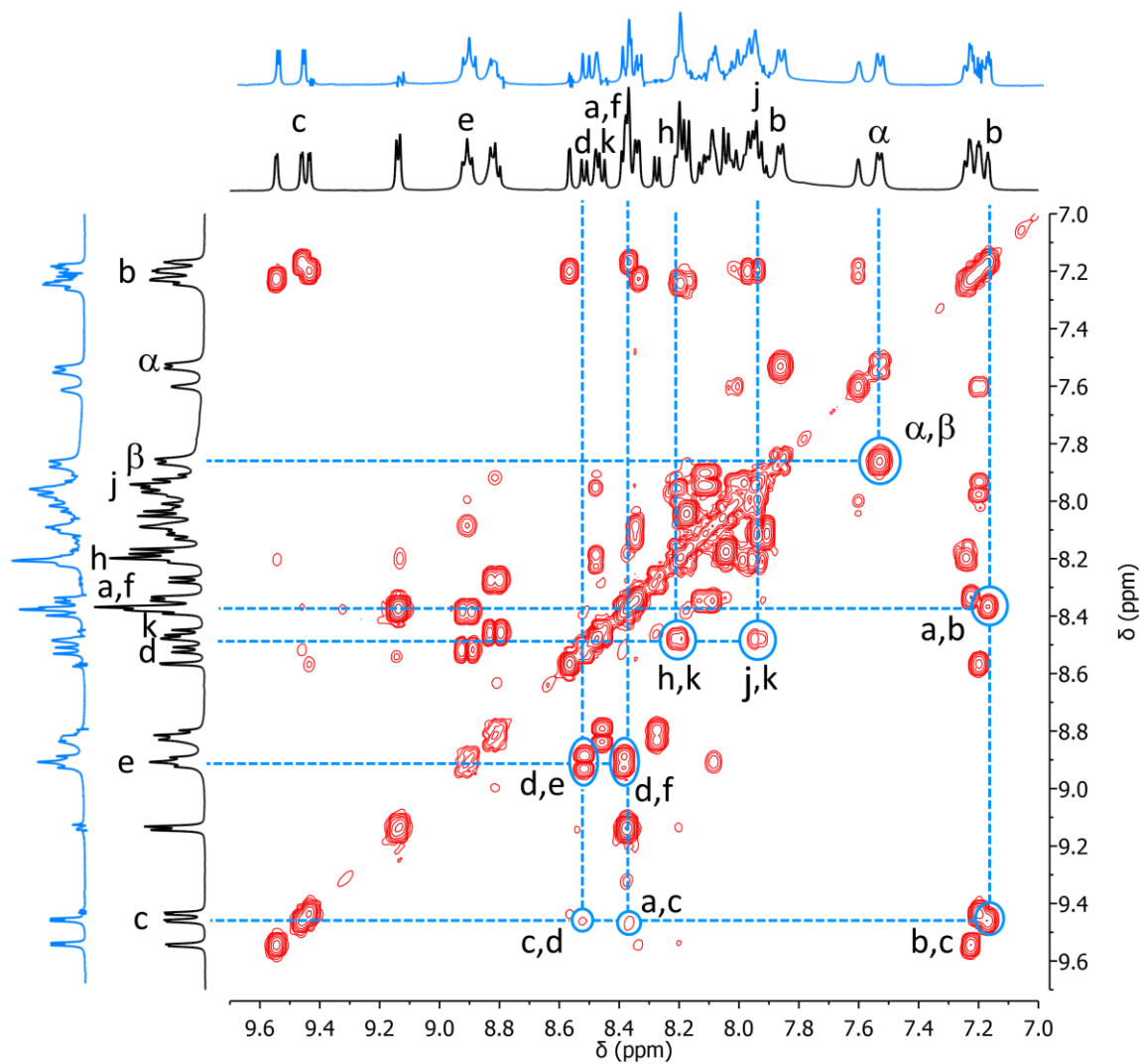


Figure 3.6 Partial ^1H COSY NMR spectrum (500 MHz, $[\text{D}_6]$ DMSO, 298 K) from the equilibrium mixture of $\text{Pd}_2'\text{Pd}_2'$ and Pd_2' , showing COSY couplings for ligand environment 1 for $\text{Pd}_2'\text{Pd}_2'$. Actual spectrum shown in black, manually subtracted spectrum for $\text{Pd}_2'\text{Pd}_2'$ shown in blue.

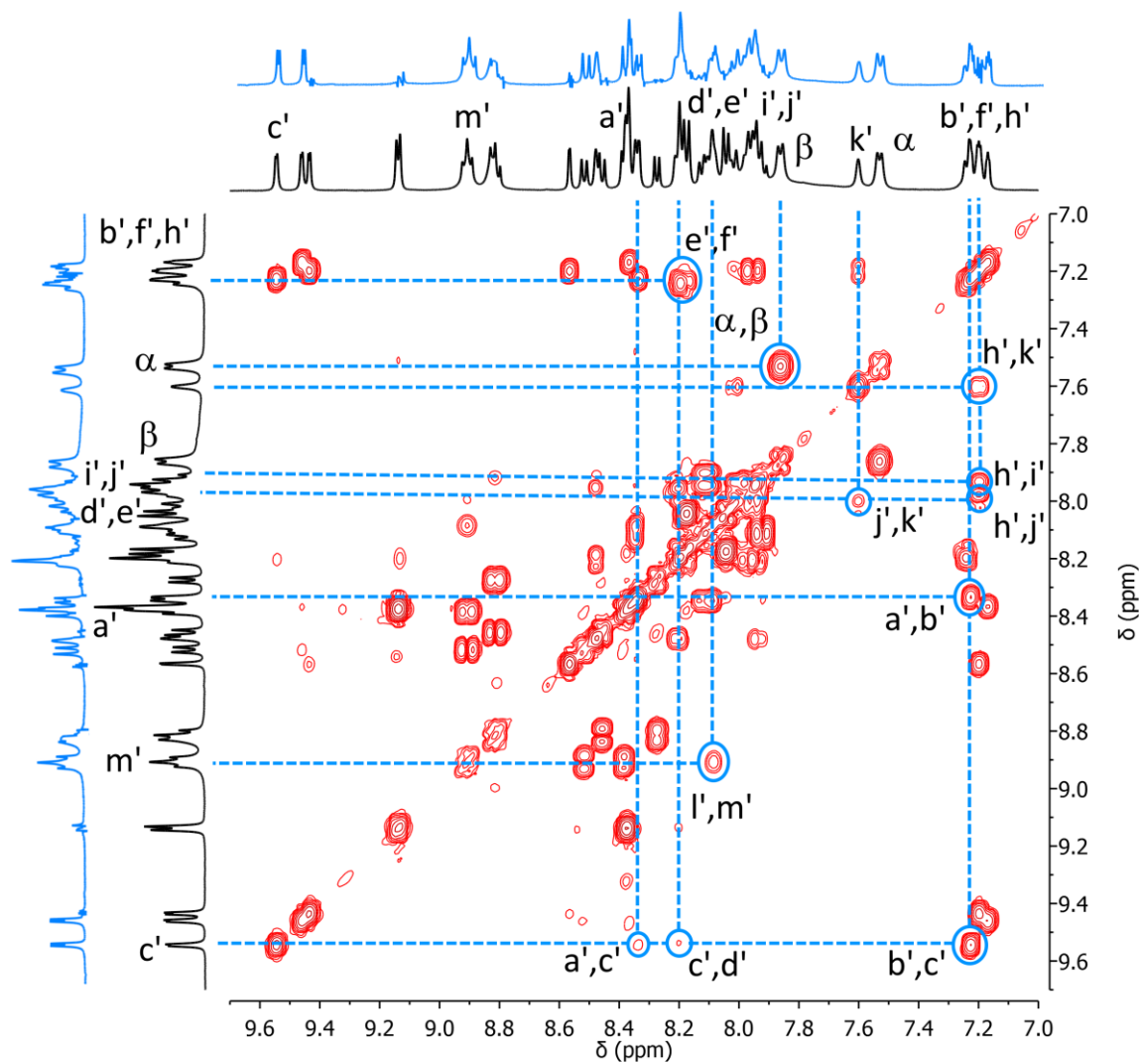
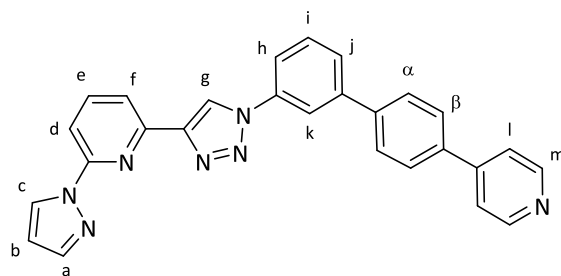


Figure 3.7 Partial ^1H COSY NMR spectrum (500 MHz, $[\text{D}_6]$ DMSO, 298 K) from the equilibrium mixture of $\text{Pd}_2'\text{Pd}_2'$ and Pd_2' , showing COSY couplings for ligand environment 2 for $\text{Pd}_2'\text{Pd}_2'$. Actual spectrum shown in black, manually subtracted spectrum for $\text{Pd}_2'\text{Pd}_2'$ shown in blue.



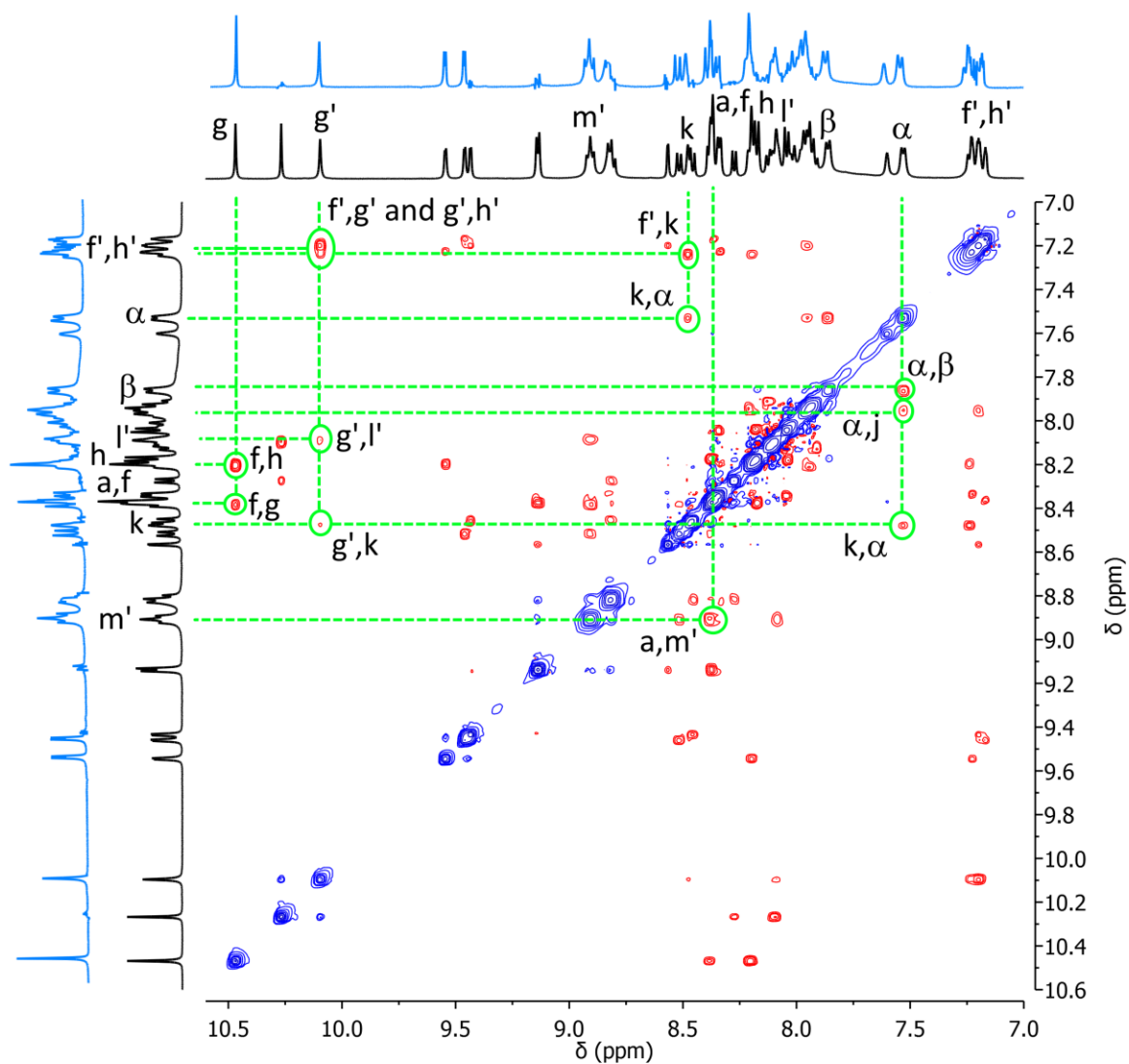
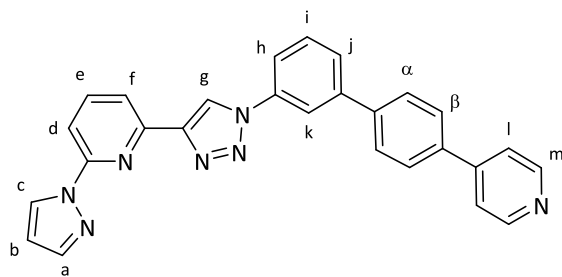


Figure 3.8 Partial ^1H ROESY NMR spectrum (500 MHz, $[\text{D}_6]$ DMSO, 298 K) from the equilibrium mixture of $\text{Pd}_2'\text{Pd}_2'$ and Pd_2' , showing key ROE couplings for $\text{Pd}_2'\text{Pd}_2'$. Actual spectrum shown in black, manually subtracted spectrum for $\text{Pd}_2'\text{Pd}_2'$ shown in blue.



3.2 Incomplete conversion to catenane $\text{Pt}_2'\text{Pt}_2'$

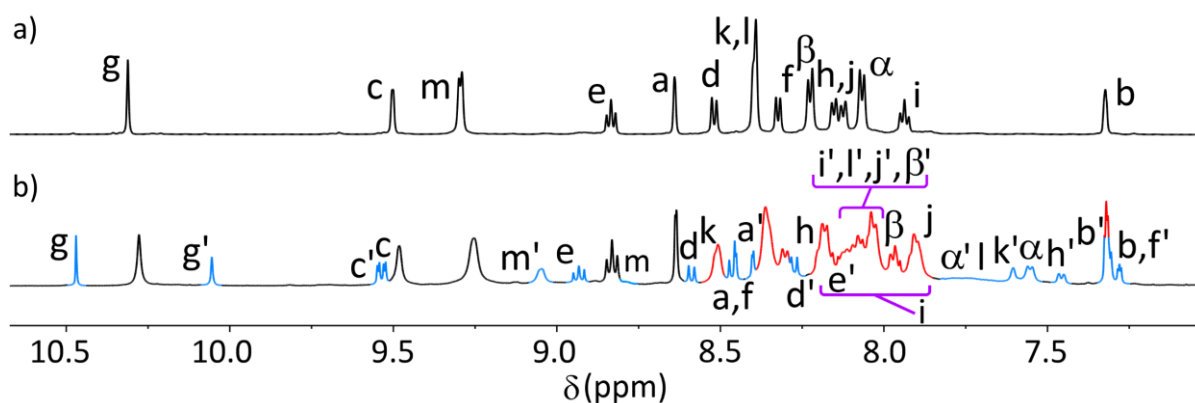


Figure 3.9 a) Pt_2' , and b) an equilibrium mixture of Pt_2' and $\text{Pt}_2'\text{Pt}_2'$ at $[\text{L}'] = 60$ mM, (colours: black, Pt_2' ; blue, $\text{Pt}_2'\text{Pt}_2'$; red overlapping peaks from both species). For assignments of $\text{Pt}_2'\text{Pt}_2'$ species in spectrum b, the labels without dashes pertain to the 'outermost' ligands in the catenane, while those with dashes pertain to the 'innermost'.

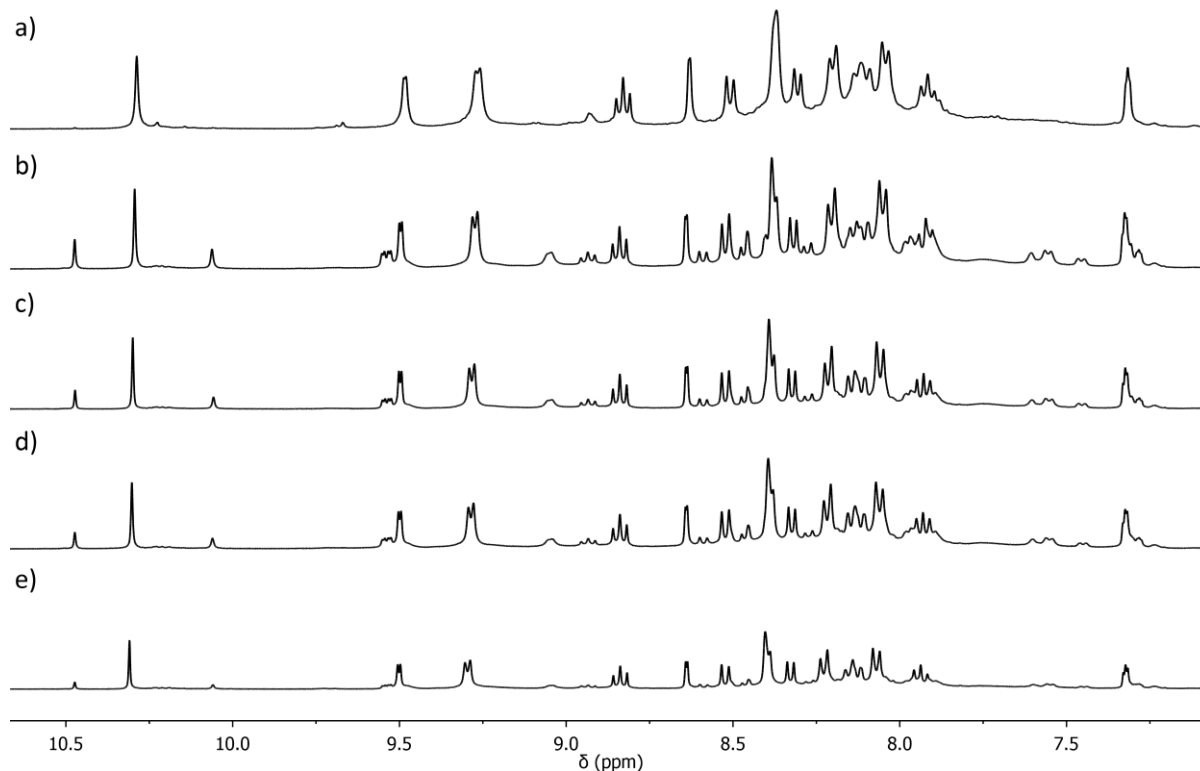
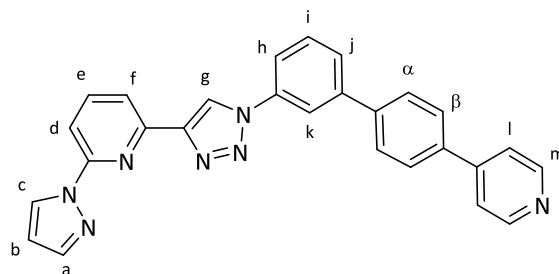


Figure 3.10 Partial ^1H NMR stacked spectra (400 MHz, $[\text{D}_6]$ DMSO, 298 K) of a 2:2 mixture of L' and Pt^{II} at $[\text{L}'] = 100$ mM, after a) 1 day at 120 $^\circ\text{C}$, then (as Pt_2' precipitates) after b) another 1 day, c) 2 days, d) 3 days, and e) 8 days.

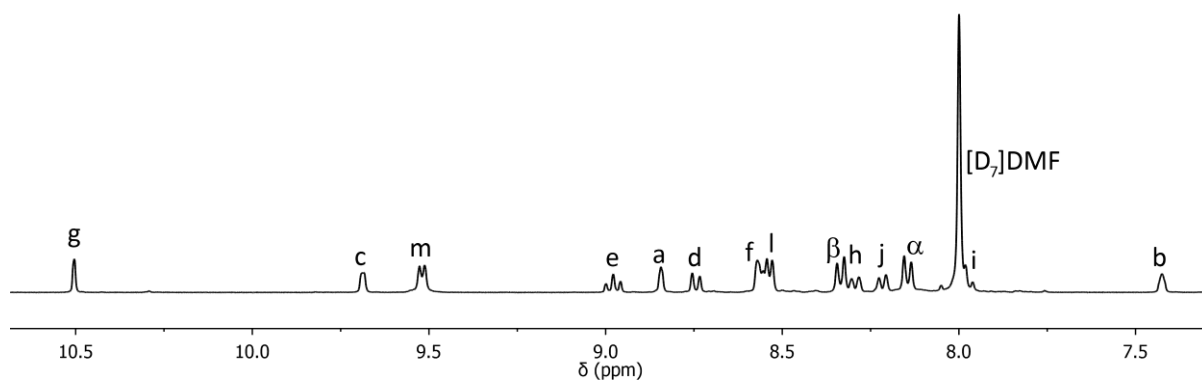


Figure 3.11 Partial ^1H NMR spectrum (400 MHz, $[\text{D}_7]\text{DMF}$, 298 K) from precipitate from mixture of Pt_2' and $\text{Pt}_2'\text{Pt}_2'$ (dissolved without heat), consistent with Pt_2' .

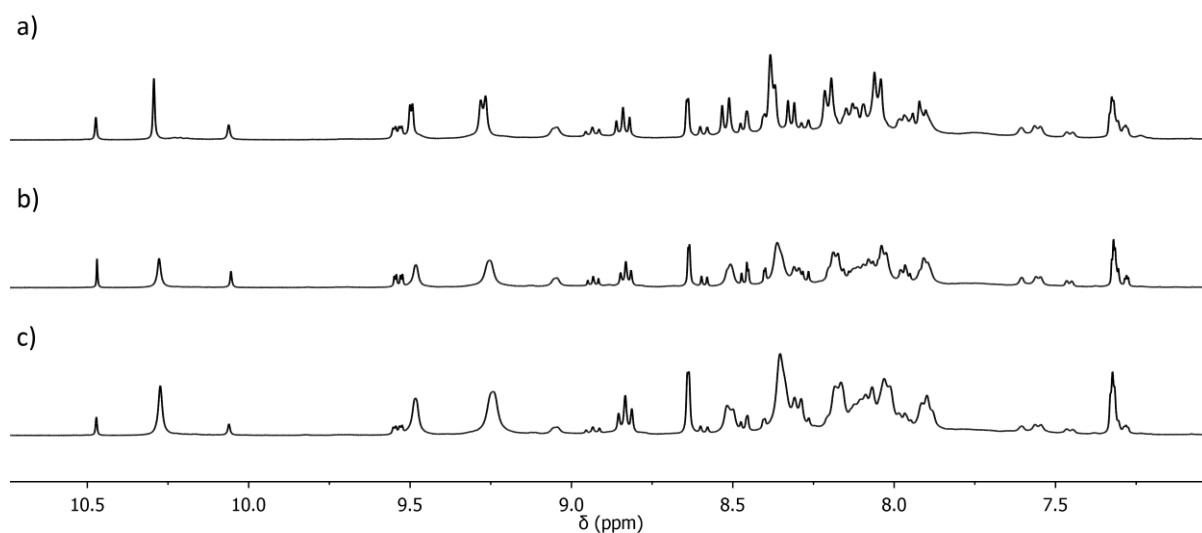


Figure 3.12 Partial ^1H NMR stacked spectra (400 MHz, $[\text{D}_6]\text{DMSO}$, 298 K) of a 2:2 mixture of L' and Pt^{II} showing the maximum observed proportion of $\text{Pt}_2'\text{Pt}_2'$, at a) $[\text{L}'] = 100$ mM (1 day), b) $[\text{L}'] = 60$ mM (8 hours) and c) $[\text{L}'] = 30$ mM (2 days).

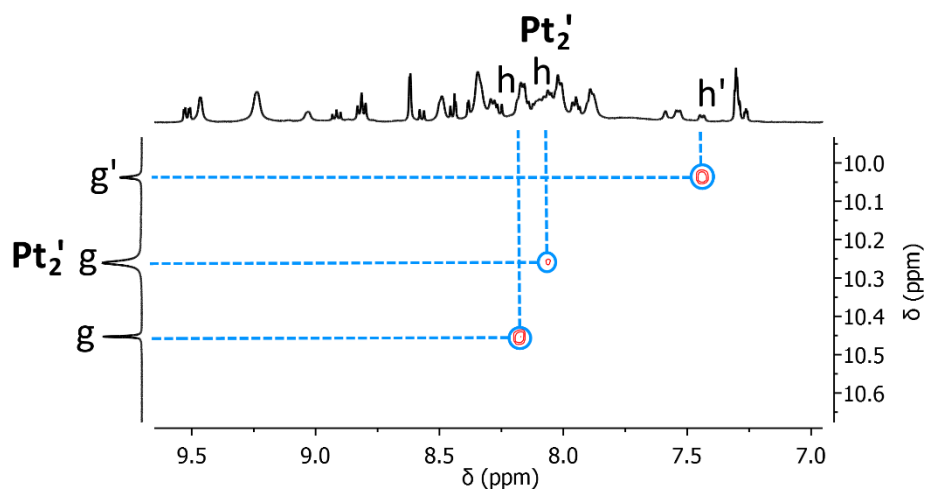


Figure 3.13 Partial ^1H COSY NMR spectrum (500 MHz, $[\text{D}_6]\text{DMSO}$, 298 K) from the equilibrium mixture of $\text{Pt}_2'\text{Pt}_2'$ and Pt_2' , showing COSY couplings between H_g proton environments and H_h proton environments.

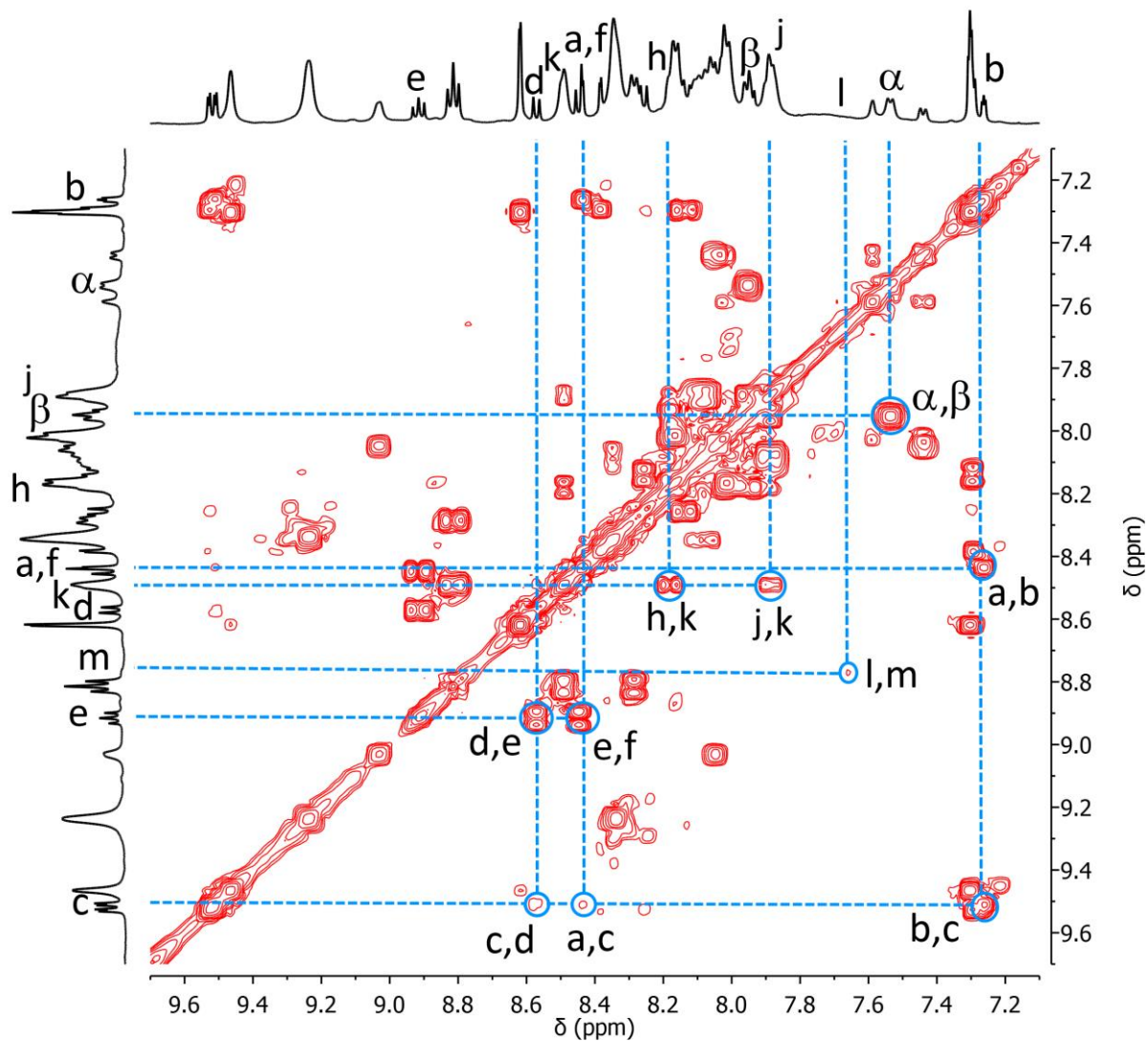
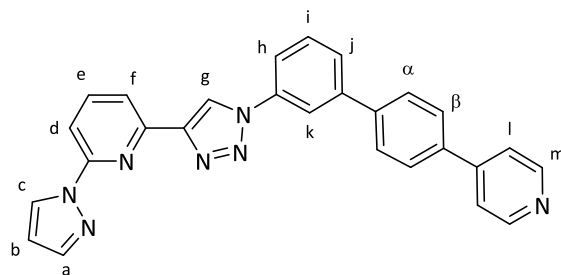


Figure 3.14 Partial ^1H COSY NMR spectrum (500 MHz, $[\text{D}_6]$ DMSO, 298 K) from the equilibrium mixture of $\text{Pt}_2'\text{Pt}_2'$ and Pt_2' , showing COSY couplings for ligand environment 1 for $\text{Pt}_2'\text{Pt}_2'$.



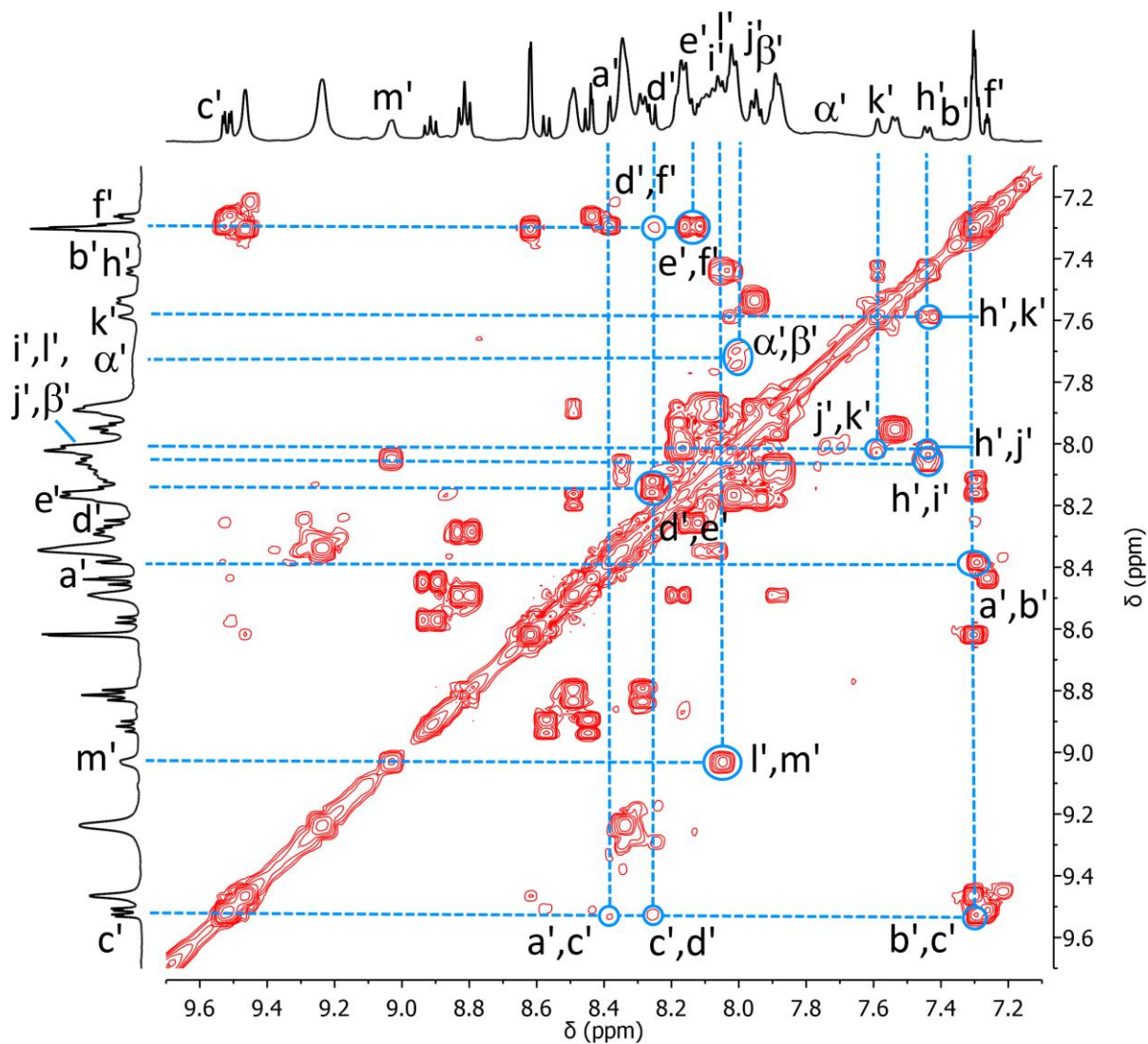


Figure 3.15 Partial ^1H COSY NMR spectrum (500 MHz, $[\text{D}_6]$ DMSO, 298 K) from the equilibrium mixture of $\text{Pt}_2'\text{Pt}_2'$ and Pt_2' , showing COSY couplings for ligand environment 2 for $\text{Pt}_2'\text{Pt}_2'$.

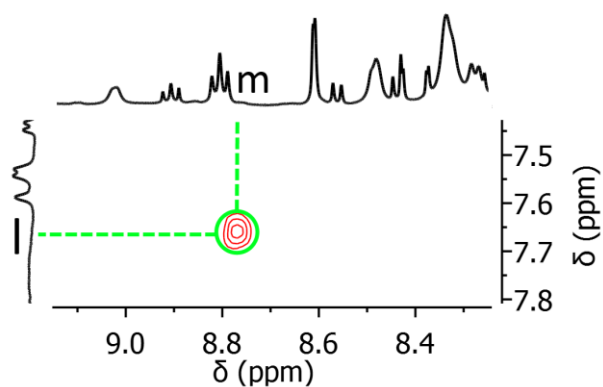


Figure 3.16 Close up ^1H TOCSY spectrum (500 MHz, $[\text{D}_6]$ DMSO, 298 K) from the equilibrium mixture of $\text{Pt}_2'\text{Pt}_2'$ and Pt_2' , confirming through-bond coupling of H_m and H_i .

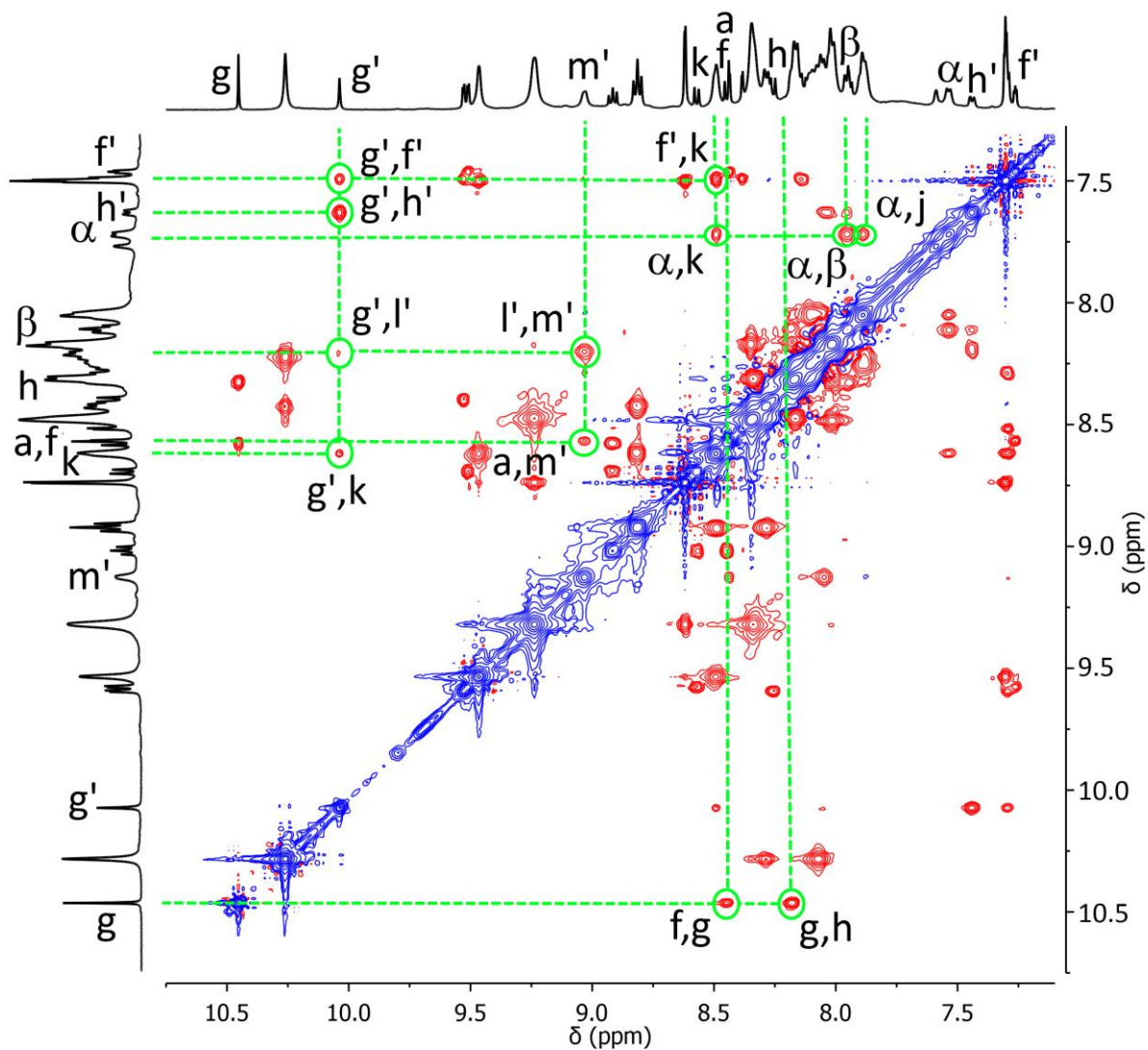
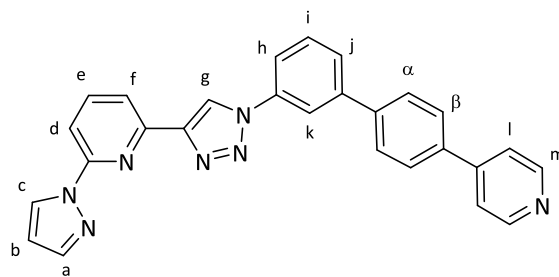


Figure 3.17 Partial ^1H ROESY NMR spectrum (500 MHz, $[\text{D}_6]$ DMSO, 298 K) from the equilibrium mixture of $\text{Pt}_2'\text{Pt}_2'$ and Pt_2' , showing key ROE couplings for $\text{Pt}_2'\text{Pt}_2'$.



3.3 Mass spectral data

Several of the $[M_2L_2]^{4+}$ dinuclear species (i.e., **Pd₂**, **Pt₂**, and **Pd₂'**, vide supra) showed small peaks in their mass spectrum (obtained under dilute conditions) when the ^1H NMR spectra from these samples showed no evidence of larger species. This is presumably due to aggregation under mass spectral conditions. It was important to rule this out in mass spectra obtained for the catenanes. For the **Pt₂'** systems, this was ensured by running spectra of quantitatively formed **Pt₂'** and of a **Pt₂'**/**Pt₂'Pt₂'** mixture under the same conditions and concentrations. Due to the greater level of inertness with Pt^{II} , this allowed direct comparison of the spectra, showing that the mixture contained a $[\text{Pt}_2\text{L}'_4]^{8+}$ cationic species, with counterions. For the **Pd₂'** system, which equilibrated rapidly, direct injection at $[\text{L}'] = 30 \text{ mM}$ was carried out. Comparison was made to a spectrum obtained for **Pd₂** under the same conditions and concentration, which showed little enhancement, in comparison, of a $[\text{M}_4\text{L}_4]^{8+}$ species (with counterions).

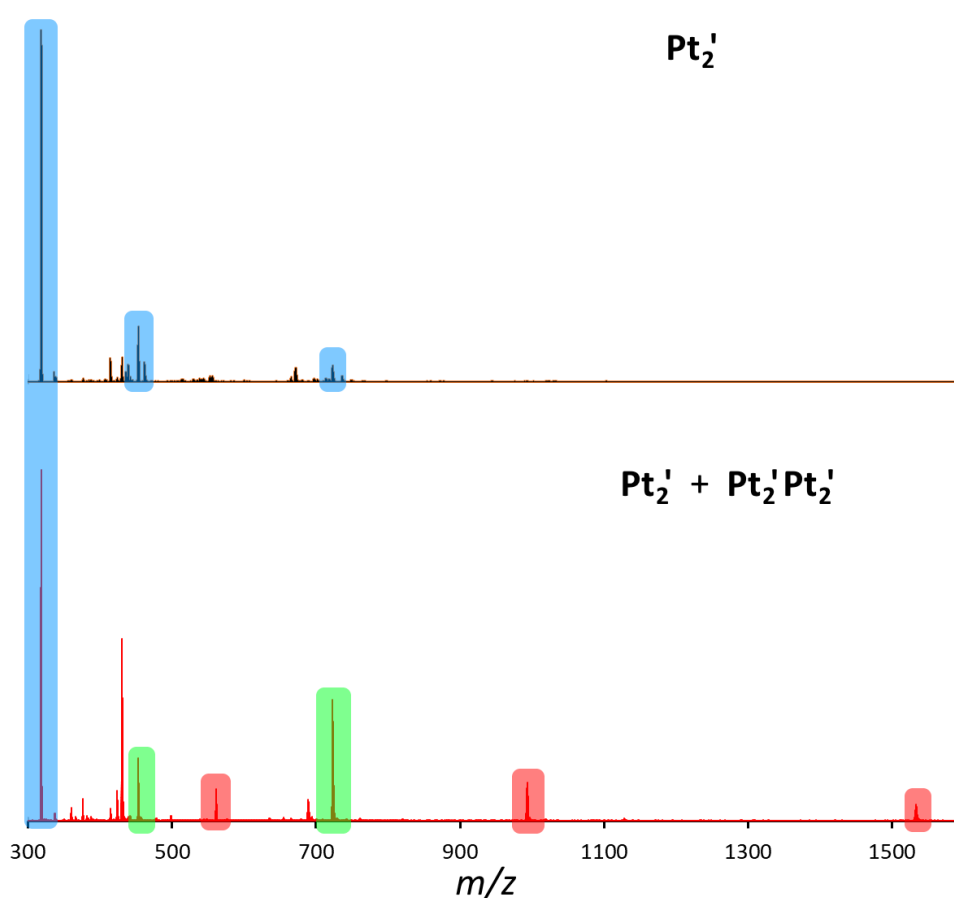


Figure 3.18 Mass spectra ($[\text{D}_6]\text{DMSO/DMF}$) of **Pt₂'** (above) and a mixture of **Pt₂'** and **Pt₂'Pt₂'**, obtained under the same concentration and method. Blue shading pertains to **Pt₂'**, red shading to **Pt₂'Pt₂'**, and green shading to overlapping peaks pertaining to both species.

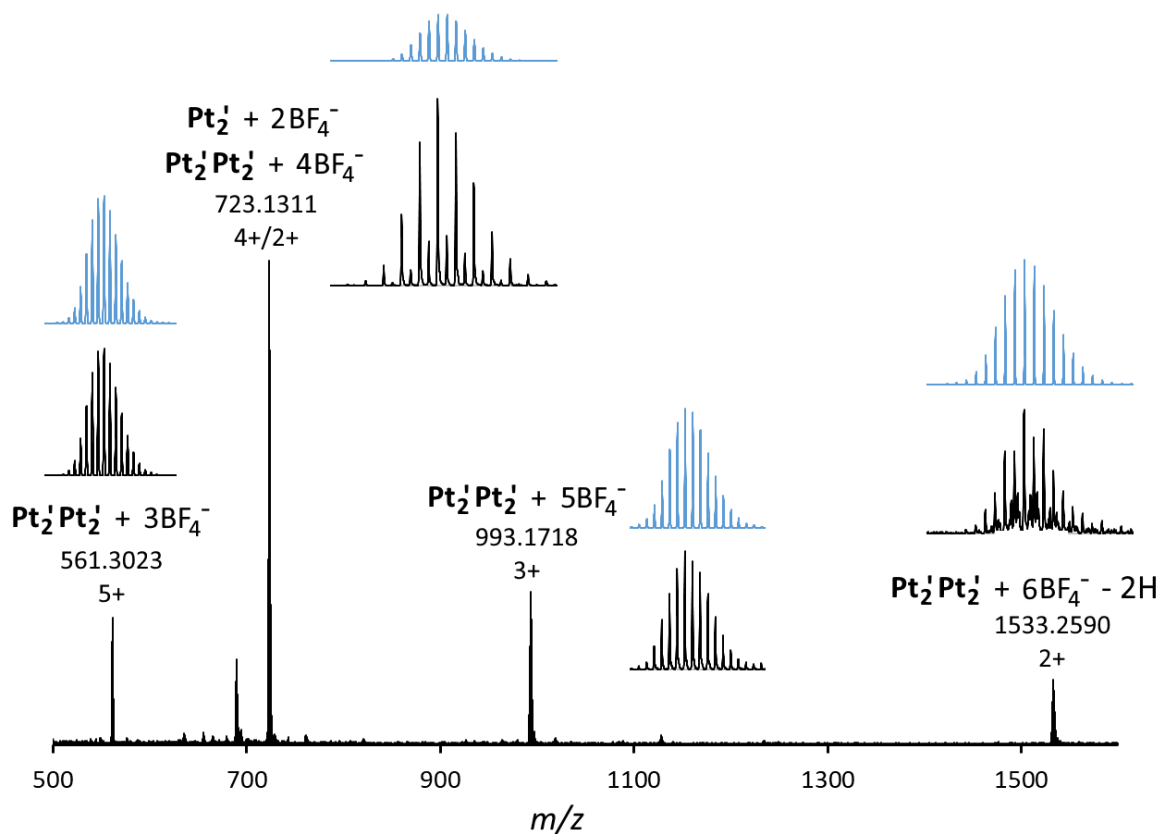


Figure 3.19 Partial mass spectrum ($[D_6]$ DMSO/DMF) of a mixture of Pt_2' and $Pt_2'Pt_2'$, showing peaks related to $Pt_2'Pt_2'$. Observed isotopic distributions shown below in black, calculated isotopic distributions above in blue.

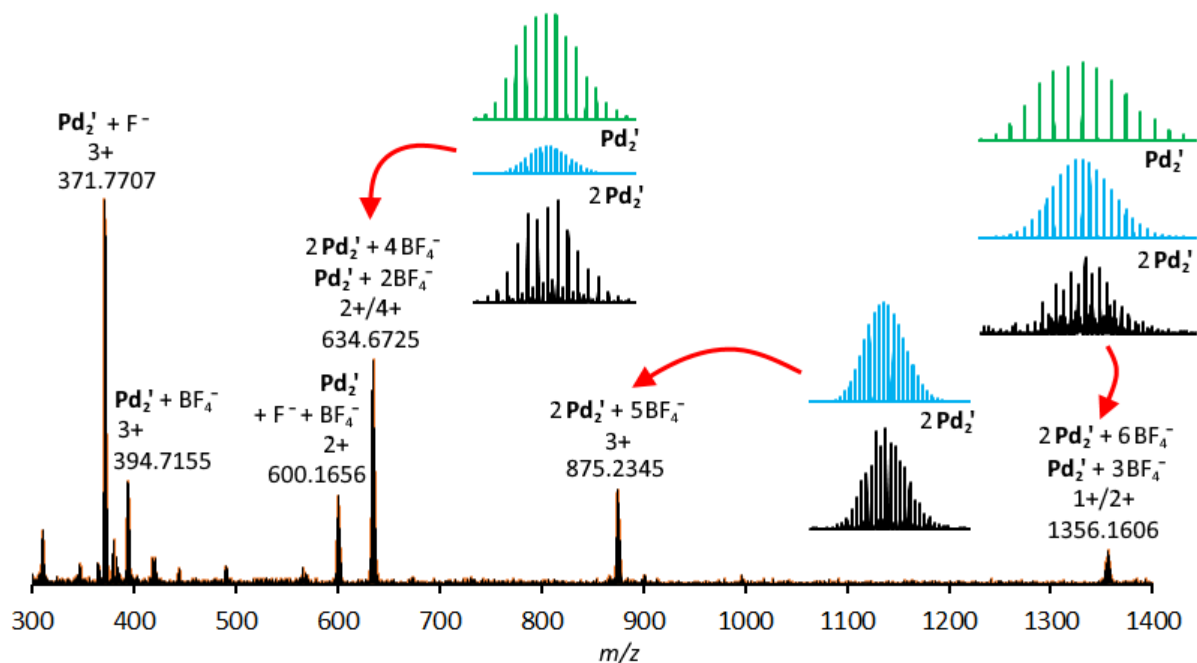


Figure 3.20 Partial mass spectrum (DMSO/DMF, direct injection at $[L'] = 30$ mM) of $Pd_2'Pd_2'$. Calculated isotopic distributions for $Pd_2'Pd_2'$ shown above in blue, those of Pd_2' in green, observed in black below. Note that cationic $[Pd_4L_4]^{8+}$ species were not obtained at significant intensity for Pd_2 under the same conditions.

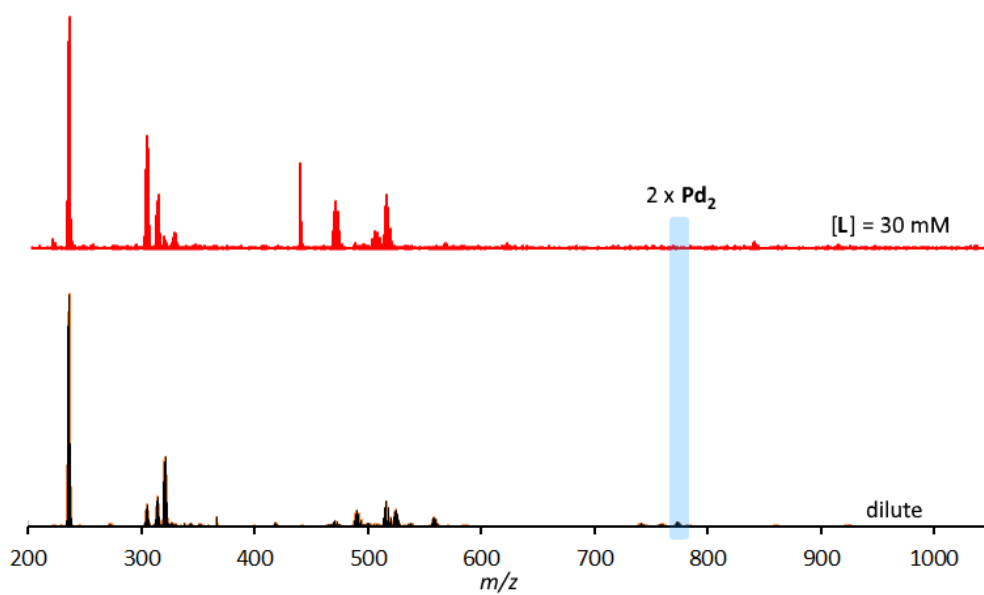


Figure 3.21 Comparison of the partial mass spectra (DMF) of Pd₂ at high concentration ([L] = 30 mM) via direct injection (red) and normal dilution (black). Note the lack of significant enhancement of the [Pd₄L₄ + 5BF₄]³⁺ peak under direct injection.

4 ¹H DOSY NMR data

Table 4.1 Diffusion coefficients (D , $\times 10^{-10} \text{ m}^2 \text{ s}^{-1}$) derived from ¹H NMR DOSY spectroscopy (500 MHz, [D₆]DMSO, 298 K) for compounds in this study.

Species	D ($\times 10^{-10} \text{ m}^2 \text{ s}^{-1}$), for [ligand] =		
	5 mM	30 mM	60 mM
L	2.41	-	-
L'	2.06	-	-
Pd ₂	1.20	1.14	-
Pd ₂ '	1.17	1.19 ^a	1.00 ^a
Pt ₂	1.23	1.11	-
Pt ₂ '	1.16	1.04	1.08 ^a
Pd ₂ 'Pd ₂ '	-	0.92 ^a	0.74 ^a
Pt ₂ 'Pt ₂ '	-	-	0.79 ^a

^aFrom equilibrium mixtures, calculated only from peaks unambiguously pertaining to the relevant species.

4.1 Ligands

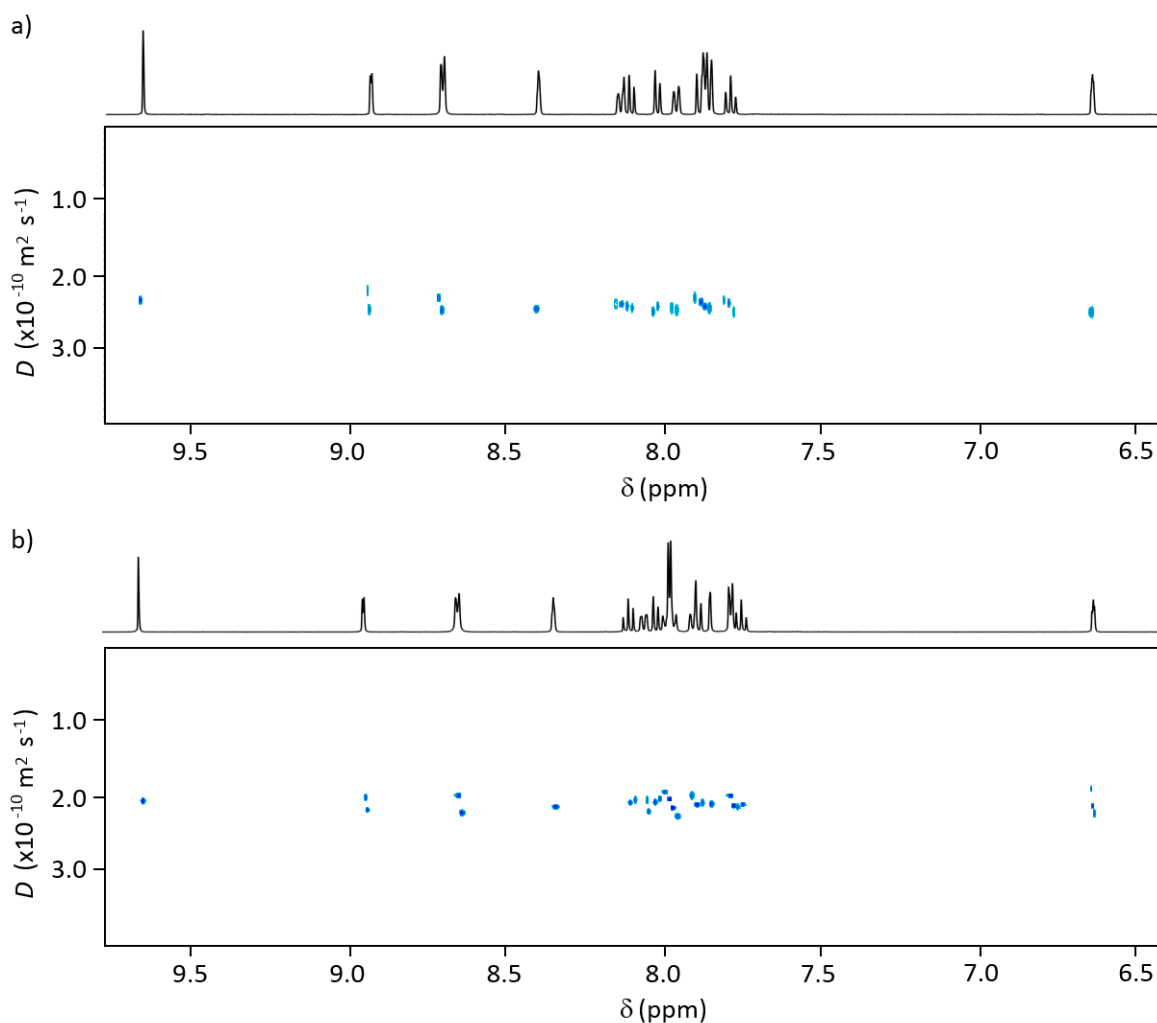


Figure 4.1 ¹H DOSY NMR spectra (500 MHz, [D₆]DMSO, 298 K) at [ligand] = 5 mM for a) L and b) L'.

4.2 Palladium(II) complexes

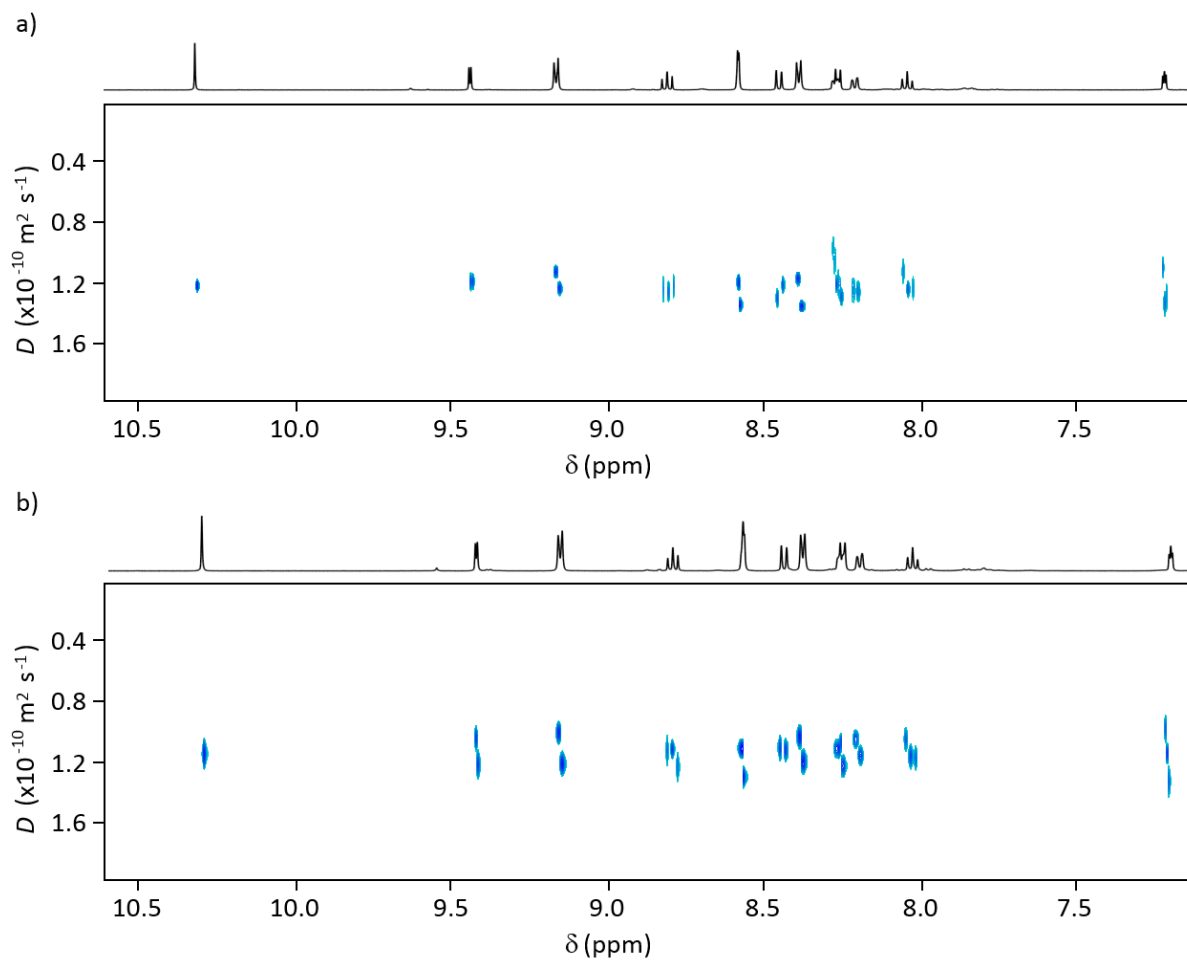


Figure 4.2 ^1H DOSY NMR spectra (500 MHz, $[\text{D}_6]$ DMSO, 298 K) for a) Pd_2 at $[\text{L}] = 5 \text{ mM}$ and b) Pd_2 at $[\text{L}] = 30 \text{ mM}$.

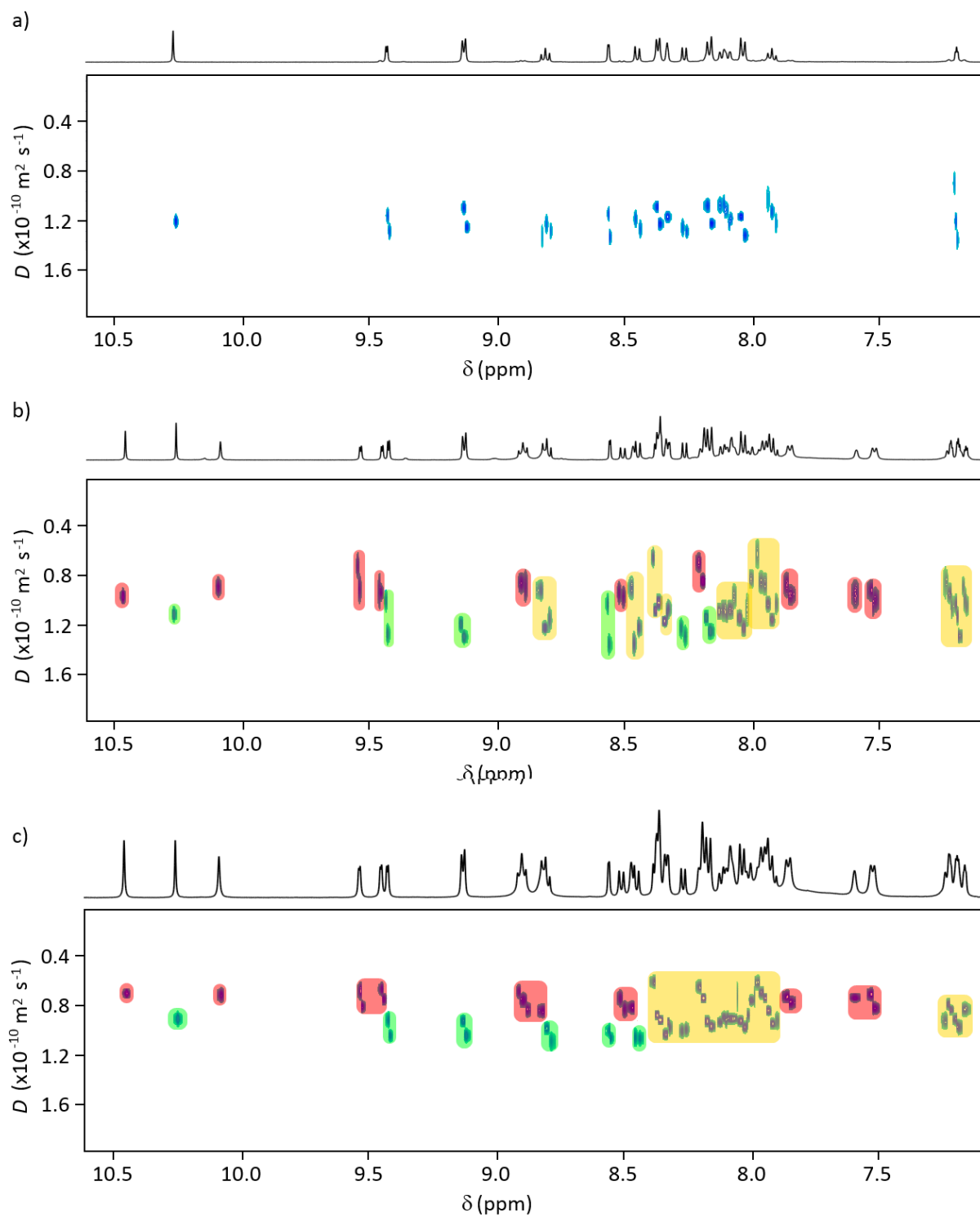


Figure 4.3 ^1H DOSY NMR spectra (500 MHz, $[\text{D}_6]$ DMSO, 298 K) for a) Pd_2' at $[\text{L}'] = 5 \text{ mM}$, b) Pd_2 and $\text{Pd}_2'\text{Pd}_2'$ at $[\text{L}'] = 30 \text{ mM}$, and c) Pd_2 and $\text{Pd}_2'\text{Pd}_2'$ at $[\text{L}'] = 60 \text{ mM}$. Colours in b and c, red $\text{Pd}_2'\text{Pd}_2'$, green Pd_2' , yellow for overlapping peaks.

4.3 Platinum(II) complexes

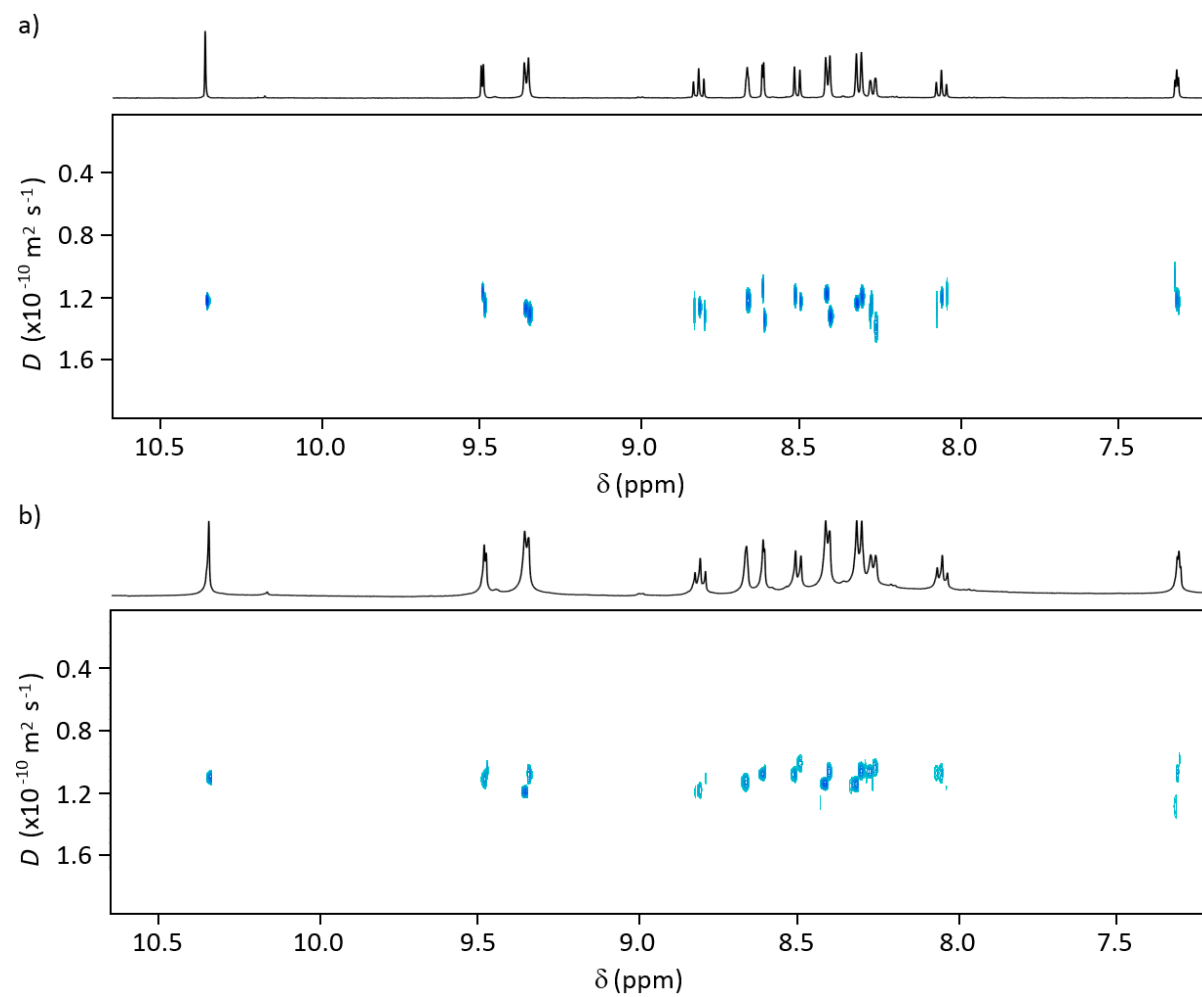


Figure 4.4 ^1H DOSY NMR spectra (500 MHz, $[\text{D}_6]\text{DMSO}$, 298 K) for a) Pt_2 at $[\text{L}] = 5$ mM and b) Pt_2 at $[\text{L}] = 30$ mM.

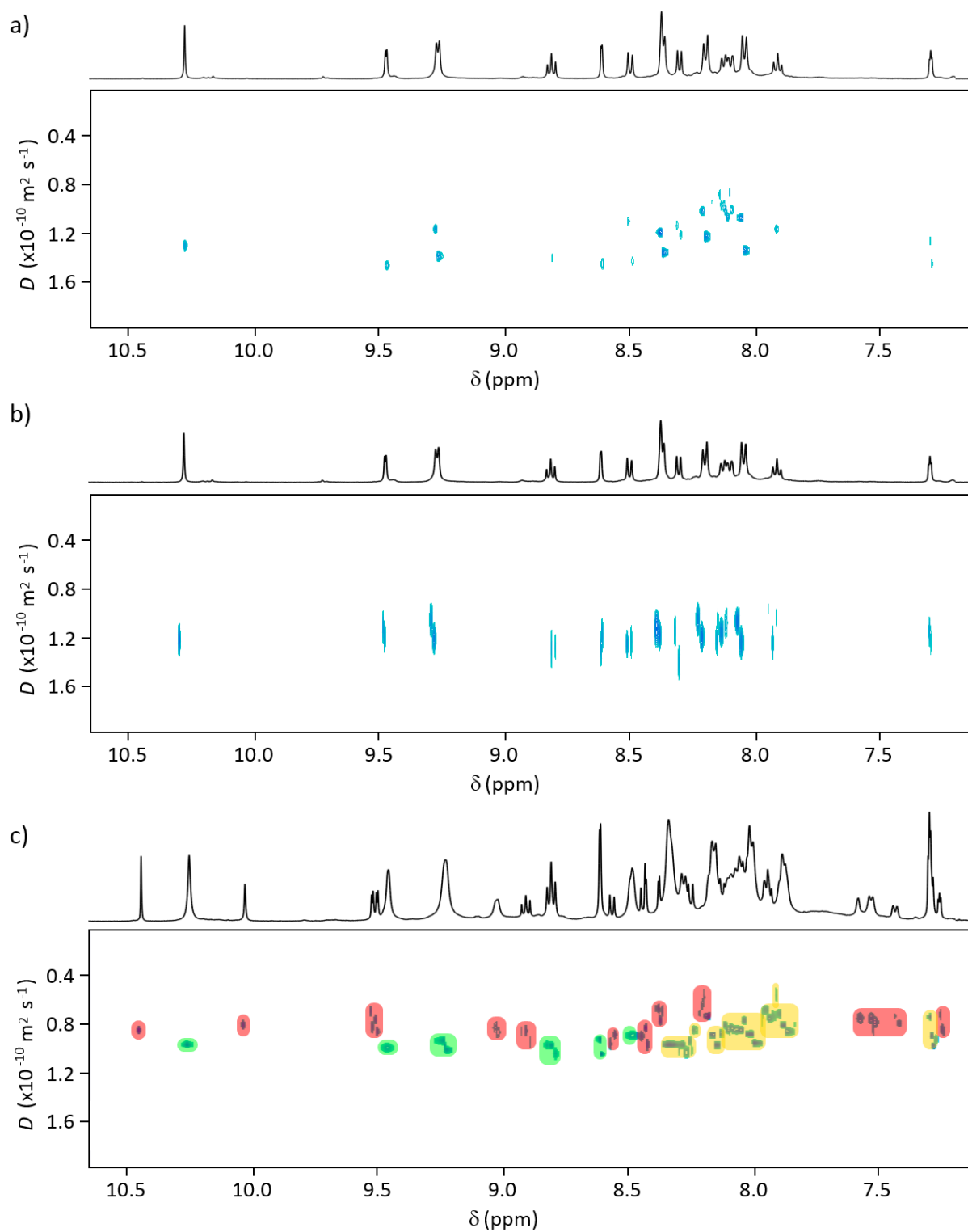


Figure 4.5 ^1H DOSY NMR spectra (500 MHz, $[\text{D}_6]\text{DMSO}$, 298 K) for a) Pt_2' at $[\text{L}'] = 5 \text{ mM}$, and b) Pt_2' at $[\text{L}'] = 30 \text{ mM}$, and c) Pt_2 and $\text{Pt}_2'\text{Pt}_2'$ at $[\text{L}'] = 60 \text{ mM}$. Colours in c), red $\text{Pt}_2'\text{Pt}_2'$, green Pt_2' , yellow for overlapping peaks.

5 Computations

DFT calculations were performed using the ORCA program version 4.0.^[10] Structures were fully optimized using the BP86^[11] functional with a def2-SVP basis set.^[12] The resolution of identity approximation^[13] was also used in the BP86 calculations, with a def2-SVP/J auxiliary basis set.^[14] Calculations were performed in a polarizable continuum solvent using the COSMO^[15] solvation model with DMSO ($\epsilon = 47.2000$). SCF iterations were considered converged when the energy change was less than 1×10^{-8} a.u. The geometry was considered optimized when the following tolerances were met: maximum gradient = 3×10^{-4} a.u., RMS gradient = 1×10^{-4} a.u., maximum displacement = 4×10^{-3} a.u., RMS displacement = 2×10^{-3} a.u., To reduce numerical error in the DFT integration, more grid points were used for both the angular and radial grids via the keyword "Grid4" for the SCF iterations and "Grid5" for the final energy evaluation. The energetic difference between the two optimised structures was 4.5 kJ mol^{-1} . Optimised structures are available as xyz files.

6 References

- [1] Y. Lu, L. Wang, X. Wang, T. Xi, J. Liao, Z. Wang, F. Jiang, *Eur J Med Chem* **2017**, *135*, 125-141.
- [2] T. Li, L. Guo, Y. Zhang, J. Wang, Z. Li, L. Lin, Z. Zhang, L. Li, J. Lin, W. Zhao, J. Li, P. G. Wang, *Carbohydr. Res.* **2011**, *346*, 1083-1092.
- [3] T. Song, X. Rao, Y. Cui, Y. Yang, G. Qian, *J. Alloys Compd.* **2013**, *555*, 22-27.
- [4] S.-J. Su, D. Tanaka, Y.-J. Li, H. Sasabe, T. Takeda, J. Kido, *Org. Lett.* **2008**, *10*, 941-944.
- [5] N. K. Allampally, M. Bredol, C. A. Strassert, L. De Cola, *Chem. - Eur. J.* **2014**, *20*, 16863-16868.
- [6] in *CrysAlisPro*, Agilent Technologies, Yarnton, England, **2012**.
- [7] G. M. Sheldrick, *Acta Crystallogr., Sect. A: Found. Crystallogr.* **2008**, *64*, 112-122.
- [8] O. V. Dolomanov, L. J. Bourhis, R. J. Gildea, J. A. K. Howard, H. Puschmann, *J. Appl. Crystallogr.* **2009**, *42*, 339-341.
- [9] in *Spartan '16*, Wavefunction, Inc., Irvine, CA, **2016**.
- [10] F. Neese, *Wiley Interdisciplinary Reviews: Computational Molecular Science* **2012**, *2*, 73-78.
- [11] a) A. D. Becke, *Physical Review A* **1988**, *38*, 3098-3100; b) J. P. Perdew, *Physical Review B* **1986**, *33*, 8822-8824; c) J. P. Perdew, W. Yue, *Physical Review B* **1986**, *33*, 8800-8802.
- [12] A. Schäfer, H. Horn, R. Ahlrichs, *The Journal of Chemical Physics* **1992**, *97*, 2571-2577.
- [13] F. Neese, *Journal of Computational Chemistry* **2003**, *24*, 1740-1747.
- [14] a) K. Eichkorn, O. Treutler, H. Oehm, M. Haeser, R. Ahlrichs, *Chem. Phys. Lett.* **1995**, *240*, 283-290; b) K. Eichkorn, O. Treutler, H. Oehm, M. Haeser, R. Ahlrichs, *Chem. Phys. Lett.* **1995**, *242*, 652-660; c) K. Eichkorn, F. Weigend, O. Treutler, R. Ahlrichs, *Theor. Chem. Acc.* **1997**, *97*, 119-124.
- [15] a) J. Andzelm, C. Kolmel, A. Klamt, *J. Chem. Phys.* **1995**, *103*, 9312-9320; b) A. Klamt, V. Jonas, *J. Chem. Phys.* **1996**, *105*, 9972-9981; c) A. Klamt, G. Schueuermann, *J. Chem. Soc., Perkin Trans. 2* **1993**, 799-805.